Towards nanomedicines of the future: Remote magneto-mechanical actuation of nanomedicines by alternating magnetic fields⋆

Yuri I. Golovin[a,b], **Sergey L. Gribanovsky**[a], **Dmitry Y. Golovin**[a], **Natalia L. Klyachko**[b,d], **Alexander G. Majouga**[b,c], **Alyssa M. Master**[d], **Marina Sokolsky**[d], and **Alexander V. Kabanov**[b,d,*]

[a]Nanocenter, G. R. Derzhavin Tambov State University, Tambov 392000, Russian Federation

[b]Laboratory of Chemical Design of Bionanomaterials, Faculty of Chemistry, M. V. Lomonosov Moscow State University, Moscow, 117234, Russian Federation

[c]National University of Science and Technology MISiS, Leninskiy pr., 9, Moscow 119049, Russian Federation

[d]Center for Nanotechnology in Drug Delivery, UNC Eshelman School of Pharmacy, University of North Carolina at Chapel Hill, NC 27599, USA

Abstract

The paper describes the concept of magneto-mechanical actuation of single-domain magnetic nanoparticles (MNPs) in super-low and low frequency alternating magnetic fields (AMFs) and its possible use for remote control of nanomedicines and drug delivery systems. The applications of this approach for remote actuation of drug release as well as effects on biomacromolecules, biomembranes, subcellular structures and cells are discussed in comparison to conventional strategies employing magnetic hyperthermia in a radio frequency (RF) AMF. Several quantitative models describing interaction of functionalized MNPs with single macromolecules, lipid membranes, and proteins (*e.g.* cell membrane receptors, ion channels) are presented. The optimal characteristics of the MNPs and an AMF for effective magneto-mechanical actuation of single molecule responses in biological and bio-inspired systems are discussed. Altogether, the described studies and phenomena offer opportunities for the development of novel therapeutics both alone and in combination with magnetic hyperthermia.

Keywords

1. Introduction

The field of nanomedicine and drug delivery has undergone explosive development over the last decade. This development was prepared by the early work on the nanoparticulate drug carriers such as liposomes, drug–polymer conjugates, polymeric micelles, polyion complexes, and degradable nanoparticles in the 1980s and early 1990s. By the new millennium the nanomedicine and drug delivery field has become defined as a cross-section of medical, pharmaceutical, and biochemical engineering research that focuses on advanced therapeutic modalities of the base of nanomaterials ranging from about 10 nm to about 100 nm in diameter. The term "nanomedicine" that emerged in science fiction and art very rapidly became anything but fantasy as dozens of nanoscale size therapeutics received marketing approval and many more new ones have entered clinical evaluation [1–6].

From the standpoint of the drug delivery science the nanomedicine tasks include 1) efficient loading of the drugs or biomacromolecules into a nanoparticulate carrier, 2) safe delivery of the loaded carrier to the target organ and/or cell in the body, and 3) timely release of the payload. Selected nanomaterials are being themselves sought as therapeutic, diagnostic or theranostic modalities that in some cases need to be actuated at the site of the action. The first task – loading has been addressed very well, for what purpose scientists initially adopted nanoscale structures already discovered by polymer and material sciences and then followed up by invention of the whole range of new nanomaterials specifically tailored for the drug delivery purposes such as block ionomer complexes, PRINT (*P*article *R*eplication *In* Non-wetting *T*emplate) nanoparticles and others. The second task remains a field of active research and discovery, where we have lately seen some successes and setbacks. Major challenges remain such as passive and active targeting, safety, host organism immune response, avoidance or employment of the reticuloendothelial system (RES), cell transport and endosomal escape. In spite of these challenges, however, we can reliably deliver therapeutically effective doses of some major anti-cancer and other medications using nanoformulations and have shown that these formulations can improve the therapeutic index compared to non-formulated molecules. The third task has not been addressed and is the field where the advances are still superficial at best. Poor drug release at the target site has hindered liposomal and micellar drugs and arguably is a major challenge for all DNA and protein delivery [7,8]. The nanomedicines of the future should provide for controlled release of the therapeutic agents, selective induction of cancer cell apoptosis, and other tasks that can be remotely actuated once these nanomedicines reach the site of their action [9–13]. Therefore, the search for the stimuli-responsive nanocarriers and versatile means for remote actuation of the cargo is an unmet need in nanomedicine. There have been many attempts to use chemical cues to trigger the target-specific release, such as acidic pH in the tumors, low endosomal/lysosomal pH, reductive intracellular environments, and tumor specific-enzymes

(cathepsins, metalloproteases, etc.) [14–16]. However, one should admit that the fidelity and robustness of these strategies might not be sufficient to achieve the desired goals.

Alternative approaches employ physical fields such as ultrasonic and ionizing irradiation, photodynamic/photothermal treatment, or electromagnetic field that can remotely affect the nanocarriers and their environment in the body [17–22] (Fig. 1). Of these fields the electromagnetic field offers substantial benefits for nanomedicine and controlled drug delivery as a remote actuation tool. Much of the early efforts focused on the use of radio frequency (RF) magnetic field and magnetic nanoparticles (MNPs) in magnetic hyperthermia used to kill cancer cells of trigger release of the drugs from heat sensitive nanocarriers (liposomes, vesicles, dendrimers, nanogels) [23–30]. More-recently, however, the attention has begun shifting to the very distinct effects of a magnetic field exerted on MNPs, namely the magneto-mechanical phenomena, which can be observed in an alternating magnetic field (AMF) of much lower frequency and in the absence of heating [31–33]. This new direction offers in our view enormous opportunities to nanomedicine and the drug delivery field. However, its future success is critically dependent upon a deep and cross-disciplinary understanding of the biological, chemical and physical phenomena underlying the interactions of the MNPs with the electromagnetic field and surrounding polymer cell and tissue environments. In this review, we focus primarily on these interactions rather on the current and future strategies for the design of the nanomedicines incorporating MNPs. Such strategies could be very diverse and there is no doubt that the mature and resourceful nanomedicine community will employ their skills and ingenuity to exploit the existing opportunities to use these novel materials to improve human health. We hope that the present review will be of help to this community. To this end, we first discuss some general principles of the interaction of a magnetic field with biological systems. Then, we provide a brief overview of the use of MNPs in RF magnetic hyperthermia, followed by a thorough consideration of the magneto-mechanic effects that are outside and beyond the classic hyperthermia concepts. Finally, we describe some physical models both published in literature and some extensions that could be helpful in understanding the magneto-mechanic phenomena and effects of non-heating super-low and low frequency magnetic fields.

2. Basis for the effects of magnetic field on biological processes

The thermal, electrochemical and electrophoretic effects of an electric/electromagnetic field have been well known and long used in therapy [34–36]. More recently the opportunities for the use of the magnetic field have attracted considerable attention. The AMF with a frequency f below 0.1 MHz is considered safe and can penetrate tissues (>1 m), which allows effective exposure of all potential targets in the human body [37].

Of course the direct effect of a magnetic field with conventionally used inductions ($B = 0.1$–1 T) on the chemical bonds is insignificant. Such field is considered "weak" from the thermodynamic point of view as the energy $U_M \approx \mu_B B$ that such field can transmit to one electron (ion, radical, atom) is negligible compared to the energy of activation of biochemical reactions $U_a \approx 0.1$–1 eV. In fact the U_M value is several orders of magnitude less than the thermal energy $U_T \approx k_B T_R \approx 0.026$ eV at room temperature T_R (here $\mu_B = 9.274 \cdot 10^{-24}$ A $\cdot$ m^2 – the Bohr magneton; $k_B = 1.38 \cdot 10^{-23}$ J/K – the Boltzmann constant).

For example, for an electron, the paramagnetic center or radical $U_M \approx 10^{-3} U_T$ at $B = 0.5$ Т И $T_R = 300$ к. The effects of the vortex electric field at the AMF frequency $f \ll 0.1$ MHz and amplitude $B < 1$ T on the ions and electrons are also negligible. The Coulomb and Lorentz forces in this case are orders of magnitude lower than the threshold values of activation of the most sensitive biochemical systems such as ion channels and receptors of cell membranes (1 to 10 pN as measured by single molecule force spectroscopy) [38].

Therefore, the balance between the needed input and required energy of activation would make impossible any effects of magnetic fields with frequency < 0.1 MHz and amplitude < 1 T on the chemical and biochemical systems in the state of thermodynamic equilibrium. However, the biochemical reactions and processes in cells and living organisms are not in thermodynamic equilibrium. As a result, the AMF and accompanying vortex electric field can affect the biochemical processes through several theoretically justified and experimentally validated mechanisms [39–43].

One extensively studied and well-established mechanism is based on spintronics. It involves the effect of the weak magnetic fields on the evolving, short-living thermodynamically unstable states of the spin subsystem that can take place in radical chemical reactions, photoluminescence and electron transfer in non-homogeneous magnetic environment [44–49] (Fig. 2a). For several decades researches have focused on the possibility of significantly altering the kinetics and yield of the spin-dependent chemical processes in the liquid and solid phases using weak magnetic fields [44–48]. The effects of such fields on the solid-state quasi-chemical reactions, micro and macro-scale characteristics of the nonmagnetic crystals and polymers and their relaxation processes have been also well documented [50–53]. In these cases due to the lack of thermodynamic equilibrium in the evolving spin and atomic subsystems the weak magnetic field acts as a "catalyst" of sorts. It does not contribute to the total energy of the system but can change the spin state of the short living radical or ion–radical pair and as a result of inter-combinational transitions reduce spin-prohibition to the reaction processes that would not be possible in the absence of the field. Thereby the magnetically induced spin conversion leads to changes in the reaction rate constants, the yields and ratios of the reaction products. However, several strict kinetic conditions need to be met for spin conversion to proceed and it appears that meeting those conditions in biochemical environments, especially *in vivo*, is challenging [49].

Introducing either synthetic MNPs or natural magnetosomes in biological systems is known to amplify the effect of the magnetic field on these systems. This approach creates flexible, controllable and well-defined methods for the remote control of biochemical processes both *in vitro* and *in vivo*. Nearly all MNPs with a diameter $\ll 100$ nm are single-domain meaning in first approximation that all magnetic moments of the atoms in the crystal lattice of the particle are aligned along the same axis of easy magnetization. From the physics standpoint, the presence of such MNPs in an otherwise magnetically disordered environment (aqueous solution, cell or tissue) induces a very localized effect of the external magnetic field. Specifically, upon exposure of the magnetite (Fe_3O_4) nanoparticle with $d = 15$ nm, to a magnetic field of $B = 0.5$ T this nanoparticle acquires the energy $U_M \approx J_S \rho V_M B \approx 100$ $k_B T$ ($J_S \approx 80$ A m^2/kg – saturation magnetization of the magnetite MNP, ρ - MNP density, V_M – MNP volume). This energy is $\sim 10^5$ higher than that of the single electron or radical, which

clearly defines the potential effects of MNPs in the biological context. Two mechanisms of utilization of this energy – magnetic hyperthermia (Fig. 2b) and magneto-mechanical actuation (Fig. 2c) are considered more closely in this paper.

3. RF magnetic hyperthermia

Magnetic hyperthermia is the most extensively studied technique to utilize the energy that MNPs acquire in an AMF in therapeutic applications. The merits of hyperthermia as a means to trigger cancer cell death have been well established. The National Cancer Institute recognizes three categories of hyperthermia treatment for cancer: localized, regional and whole body hyperthermia [54]. Localized hyperthermia involves exposure of the tumor to high temperatures (>43 °C) to enact cell destruction and tumor regression [55]. Exposure to $T = 43–46$ °C induces apoptosis and ablation of cancer cells. A temperature increase above 46 °C induces necrosis, which can cause general system intoxication [24–26,56,57].

MNP mediated hyperthermia involves the administration of nanoparticle-based colloidal dispersions followed by application of an external AMF exposure. Heat generation of magnetic hyperthermia is caused by the interaction of the applied AMF and the magnetic moments of the MNPs [27]. Nanoparticles below 100 nm can be thought of as a single magnetic dipole whose response to an alternating magnetic field occur primarily through two mechanisms referred to as Neel and Brown relaxations (Supplementary material 1). Neel relaxation is caused by the movement of the magnetic moments relative to the crystal lattice structure of the single-domain MNP. In contrast, Brown relaxation involves the movement of the MNP relative to the surrounding medium [24]. The dissipation of the magnetic energy as a result of these processes results in the heat release, which can be quantified as the amount of the generated heat – Specific Absorption Rate (SAR). The parameters of and duration of exposure to the AMF, the MNP composition, size and shape, the MNP local concentration and aggregation state, all affect SAR. Therefore, both the applied field and the MNPs must fit certain criteria to cause hyperthermia.

3.1. Properties of the MNPs for magnetic hyperthermia

When designing a nanoparticle system for use in magnetic hyperthermia there are several criteria that should be considered. The most obvious criterion for biomedical applications is lack of intrinsic cytotoxicity. The lack of toxicity and ease of clearance have made magnetite and maghemite (γ-Fe$_2$O$_3$) the focus of most MNP studies. However, the techniques required to produce maghemite are very complex making magnetite a more suitable choice of material [55].

The magnetic properties of MNPs are very strongly correlated to their size, morphology and structure making the method of synthesis incredibly important. The synthesis technique should allow for good control over particle size, size distribution and shape [54]. In addition, the technique should yield highly reproducible results. There are several techniques used to synthesize MNPs including co-precipitation, thermal decomposition, microemulsion and sol–gel with co-precipitation and thermal decomposition being the most common [54]. The general approach to MNP synthesis requires the nucleation stage to occur before and independently of the growth stage to yield particles that are or close to monodisperse. The

most common method of chemical synthesis, called the co-precipitation technique, is the simplest method because it can be completed in water, under ambient temperatures and takes less than an hour [54]. The main advantage is that the process is highly scalable and MNPs can be produced in large quantities of relatively narrow size distribution. However, there is a limit to the control over the size distribution and, in addition, there is little control over the particle shape [58]. Very close to monodisperse MNPs can be synthesized through thermal decomposition of iron precursor compounds in high-boiling organic solvents in the presence of surfactants [54]. The obvious disadvantages of this synthesis approach are the high temperatures needed and the amount of time it takes for the reaction to finish. However, the extreme control over size along with the scalability of this technique make it ideal for biomedical applications [59].

The magnetic characteristics of MNPs depend on their submicron core size [60]. Generally, maximal SAR is observed when the relaxation time determined by the MNP composition and size is equal to the inverse frequency of the AMF. Studies have shown that the SAR of magnetite nanoparticles decreases as the nanoparticle diameter increases above 50 nm [61]. Thus, in order to achieve more efficient magnetic hyperthermia, many studies focused on particles below this 50 nm threshold. The heating capacity of maghemite particles in a RF AC field is also very strongly correlated with nanoparticle size, with the more efficient heating occurring with particles of 14–16 nm in diameter [61]. Such dependence on size is evidence that the predominant mechanism of heat generation is Neel relaxation because it characteristic time is exponentially dependent upon the volume of the MNPs. In contrast, the characteristic time of the Brown relaxation is less dependent upon particle size and the power dissipation *via* Brown relaxation becomes predominant with particles of larger diameter. This size dependence makes the MNP uniformity very important because broad size distributions make the proportion of heat generating particles smaller.

MNPs synthesis technique and coating have been shown to have a very important effect on SAR but these effects and their underlying mechanisms have not been thoroughly elucidated. A large body of *in vitro* work has been done using MNPs of varying compositions and synthesis techniques. MNPs with magnetite cores make up the majority of the work. For example, Guardia et al. synthesized nanocubes coated in polyethylene glycol (PEG) using thermal decomposition to achieve approximately 50% cell death in cancer cells by increasing the cellular temperature to 43 °C for up to an hour post-treatment [62]. In a similar fashion Samanta et al. utilized the co-precipitation technique to synthesize magnetite core nanoparticles coated in bovine serum albumin [63]. These nanoparticles with an average diameter of 28 nm were used to provide efficient heating and hyperthermia in HeLa cells while producing little cytotoxicity in the absence of an AC magnetic field [63]. Maghemite is also a popular choice for a core material when designing MNPs though as stated earlier, the synthesis methods involved with maghemite are slightly more complex. Le Renard et al. have developed an *in situ* forming polymer gel system with entrapped silica microparticles and MNPs. They synthesized the maghemite nanoparticles using the sol–gel technique and studied the heating efficiency of the system after exposure to a RF magnetic field [64]. Many of the *in vitro* MNP systems suffer from in-sufficient cellular uptake that leads to a less pronounced cytotoxicity. To combat this, Sonvico et al. developed folate-targeted maghemite nanoparticles. They developed dextran and PEG coated nanoparticles

via the co-precipitation technique followed by folate conjugation using standard N-hydroxysuccinimide chemistry. They were able to achieve very high cellular uptake particularly in folic acid overexpressing cell lines [65]. Unconventional uses of magnetic hyperthermia have also been explored. For example, Huang et al. successfully used ferrite nanoparticles to remotely control the temperature sensitive TRPV1 ion channel [66]. A more detailed review on the methods of preparation of the MNPs and the recent advances of their uses in the magnetic hyperthermia can be found elsewhere [54,67].

3.2. Field requirements for magnetic hyperthermia

Magnetic hyperthermia requires MNPs that can release heat when exposed to an AMF of sufficient frequency and strength. The temperature of the surrounding tissue must increase above 42 °C for at least 30 min to induce subsequent cell death [67]. Energy is absorbed by the MNPs and dissipated as heat by one of mechanisms mentioned previously. These mechanisms occur due to interaction between the magnetic component of the applied electromagnetic field and the magnetic moments of the MNPs. Therefore, the design of the field space is very important for achieving efficient hyperthermia.

The magnetic field strength and frequency are two parameters that vary wildly across much of the current MNP work. Generally the product of the field frequency and intensity of the magnetic field (in the absence of MNPs) should not exceed the threshold of $4.85 \cdot 10^8$ A · m^{-1} s^{-1}, which is considered safe and avoids significant eddy current heating in healthy tissue [68]. According to well-known equations governing power loss density and specific loss power, there is a linear dependence on frequency and a square relationship with amplitude of the applied field [56]. Since the heat generation by MNPs during the exposure to an AMF as a first approximation is proportional to frequency f the custom approach to magnetic hyperthermia utilizes fields with a frequency of $100 < f < 800$ kHz. An AMF with a frequency above 1 MHz generates non-specific heating of the surrounding tissues due to eddy currents and dielectric losses. In addition, at very high frequencies the thermal losses become frequency independent and are instead dependent upon the square of the field strength [56]. Below 100 kHz frequency at commonly used field strengths $B = 10$–20 mT, it appears that MNPs generate insufficient heating effects and thus, these frequencies cannot be used for magnetic hyperthermia. The AMF below these frequencies can be called non-heating magnetic fields.

3.3. The concept of local heating in magnetic hyperthermia

A conventional approach to the hyperthermia aims to generate large amounts of heat to raise the temperature within entire tumor volumes. However, this approach requires relatively high local concentrations of MNPs within a tumor. Given the well-known difficulties of delivery of nanoparticles to tumors after systemic administration, and relatively limited penetration of nanoparticles within the tumor mass it may be difficult or nearly impossible to achieve sufficient tumor concentrations of MNPs after their systemic administration. This may limit the use of conventional magnetic hyperthermia to direct injections of MNPs into localized solid tumors where it has shown limited success [69].

It has been pointed out, however, that in order to kill cancer cells one needs to localize the heating within this cancer cell, which underlies the so-called concept of intracellular hyperthermia [70–74]. MNP mediated temperature increase was proposed to increase permeability of lipid vesicle membranes to induce drug release from these vesicles by the RF AMF [75]. Moreover, the localized temperature increase mediated by manganese ferrite ($MnFe_2O_4$) MNPs (6 nm in diameter) was suggested to activate a temperature-sensitive ion channel and neurons and induce a whole organism response without observable toxic response to the cells [66]. In support of this mechanism the localized (not bulk) temperature increase was measured using a fluorescence reporter molecule attached to the surface of the MNP (although it should be pointed out that the field frequency used in this study was 40 MHz and $B \approx 0.84$ to 1.25 mT) [66]. However, another study involved measurements of fluorescence of quantum dots immobilized on MNPs at a much lower frequency range ($f < 1$ MHz and ≈ 0.6 mT) to avoid dielectric heating of the water [76]. In this study no changes in the surface temperature were found as per the theoretical predictions.

The feasibility of a temperature increase within a volume of a single cell or on the surface of a nanoparticle has been discussed with certain skepticism. Thus, a theoretical study by Rabin has concluded that conditions of hyperthermia could only be met within a cluster of several cells that are densely and fully loaded with MNPs [77]. Similar considerations and conclusions based on the theoretical analysis of the thermal diffusion using the Fourier differential heat equation were presented in a number of other studies [33,78–82]. Such analysis is presented in Supplementary material 2. It generally suggests that a local temperature increase at the surface of the MNP lies in the range of 10^{-7}–10^{-6} к. Moreover, the estimates suggest that a local increase of the temperature in the center of a dense cluster of hundreds of MNPs should not exceed 10^{-4} к.

Based on these conclusions of improbable increase of intracellular temperature several authors hypothesized that the cell death and other phenomena mediated by MNPs in an AMF may involve non-thermic but still localized mechanisms of power release to the membranes and other biological structures in the vicinity of MNPs [83–85]. Such effects are considered below.

4. Observation of magneto-mechanical actuation in biological systems

Current literature provides few examples suggesting the possibility of magneto-mechanical actuation of biological systems using functionalized MNPs activated by an AMF (Fig. 3). For ease of consideration, we have subdivided these examples into two major groups. In the first group the authors initially aimed to study magnetic hyperthermia using an AMF with relatively high frequencies from 100 to 700 kHz. However, their work could not fully explain the observed effects just by the AMF-induced heating of the MNPs, and therefore they had to imply some non-thermic mechanisms. In the second, currently much smaller group, the authors deliberately used a low or super low frequency AMF to either decrease or exclude the heating (since, as to a first approximation, the heating is directly proportional to the frequency, f). In most cases the second group studies used an AMF with $f < 100$ Hz and in rare cases up to 6 kHz.

4.1. "Non-thermic" phenomena in magnetic hyperthermia

In a growing number of studies the authors initially focus on magnetic hyperthermia, but along with interpretations based on assumptions of intracellular heating also suggest that the observed phenomena could be explained by non-thermic mechanisms. For example, the studies involving dendritic cells loaded with small magnetite MNPs (13 nm magnetite core; 10^4–10^5 MNP/cell) suggested that exposure of the cells to an AMF ($B = 16$ mT, $f = 260$ kHz) results in the death of 95–98% of cells [83,86–88]. At the same time the exposure led to only a marginal increase in the temperature from 26 to 29–30 °C, which could not explain the cytotoxic effect. Neither the MNPs alone nor the AMF alone produced a cytotoxic effect. Initially, the authors suggested that the observed effect was due to the localized "intracellular" heating. However, a more recent review of their own and other published data concluded that 5 out of 12 studies involving magnetic hyperthermia did not detect an increase of the temperature that would be sufficient to kill the cells [88]. Thus, it was suggested that despite a common use of the term "magnetic hyperthermia" in different cells, under a different AMF several distinct mechanisms of cell death *via* apoptosis or necrosis could take part, including those that are not thermic or not entirely thermic.

Moreover, the paper by the group of C. Rinaldi directly suggested that MNPs and an AMF can kill cancer cells in the absence of heating [89]. In the experiment described in this study a triple negative breast cancer (TNBC) MDA-MB-468 cell culture was maintained at 37 ± 0.2 °C during the entire period of exposure to the AMF ($B = 47$ mT, $f = 233$ kHz). To target the epidermal growth factor receptor (EGFR) displayed at the surface of these cells the MNPs were conjugated to epidermal growth factor (EGF). The targeted MNPs, upon exposure to the field, produced a significant (up to 99.9%) reduction in cell viability compared to the untargeted particles. The authors noted that the increased cell death was observed without the need for the perceptible temperature rise, under the conditions when cell apoptosis could not be expected. Therefore, they suggested that there could be either a local heating mechanism resulting in denaturation of the EGFR at the MNP surface or some mechanical affect on the EGFR by the bound MNPs. In a more recent work, the same group suggested that EGF-modified MNPs in an AMF can disrupt lysosomes and induce cell apoptosis in the absence of bulk heating [85]. As a mechanistic explanation they propose energy dissipation either through heat dissipation and/or "mechanical rotation" of the MNPs in the AMF to create shear and pulling stresses in lysosomal cell membranes, which increase their permeability.

Similar results were reported in a few other studies [90,91]. In particular, the apoptosis of the mouse skin fibrosarcoma cell line was observed upon increase of the temperature from 28 °C to 33 °C during exposure of the cells to the AMF ($B = 33.5$ mT, $f = 265$ kHz, time of exposure $t_e = 10$ min) [90]. In another study HeLa cells were incubated at 37 °C with silica-coated ferromagnetic nanoparticles of manganese oxide perovskite $La_{0.56}(SrCa)_{0.22}MnO_3$ [91]. The 30 min exposure of these cells to an AMF ($B = 15$ mT, $f = 100$ kHz) resulted in cell death *via* apoptosis while the bulk temperature increase was negligible and the temperature was always below 37.6 °C.

It needs to be pointed out that most studies that reported the thermic effect being small (less than few °C) or insufficient to explain the field induced cell death, used fields with relatively

low (for magnetic hyperthermia) frequency (f = 100 to 250 kHz) and magnetic induction (B = 10 to 35 mT) along with relatively short exposure times (<1000 s). It is not surprising therefore, that these conditions reduced the heating contributions in the registered phenomena and could expose the non-thermic effects of the AMF.

The non-thermic hypotheses discussed in the above-described publications indeed have a physical rationale. MNPs subjected to a field, in addition to heating (which is due to magnetic relaxation–re-orientation of the MNP magnetic moments **μ** in the field) also undergo a mechanical effect (Fig. 2c). In a uniform AMF with induction **B** there is a rotation moment $L = \mu \times B$; in a non-uniform AMF the rotation moment is supplemented by force $F = (\mu \cdot \nabla)B$.

The study by Saville et al. has pointed out that suspensions of small (*e.g.* 20 nm in diameter) superparamagnetic MNPs if not stabilized by long polymer brushes can form linear chain-like aggregates in the presence of an applied external AMF [92]. The measurements were conducted using an AMF with f = 150 kHz and B = 60 mT. The formation of these chains may have a dramatic impact on the biological systems, by altering the capacity of the particles to transfer magnetic energy to the surrounding cells for example by disrupting intracellular organelles.

One possible non-thermic mechanism proposed by Carrey et al. is the generation of ultrasound by MNPs in the inhomogeneous AMF [84]. This work proposed a theory for the generation of ultrasound by MNPs that undergo reverse-translational motion in viscous media in the AMF. It is well known that ultrasound both in cavitation and pre-cavitation mode can induce chemical and biological effects [93–102]. Notably, these effects do not require physical attachment of the MNPs directly to the affected molecules. However, ultrasonic activation of biological systems by MNPs has some principal limitations. According to the estimates reported by Domenech et al. the generation of the ultrasound of sufficient power requires the concurrent high frequency of the AMF ($f \sim$ 1 MHz), high solution viscosity η (~1 Pa·s, that is ~10^3 times higher than that in water) and high gradient of the field (100–1000 T/m) [85]. Such combination of conditions is difficult to realize in living cells and especially in the human body. Moreover, the high gradient of the AMF should induce rapid migration and redistribution of the MNPs within the volume of the living objects, which should complicate the control over the exposure to the field and have its own unfavorable side effects. Based on this, we may draw two conclusions: 1) in most studies described above the conditions for the ultrasound effects of MNPs in the non-uniform AMF were probably not met; and 2) the use of the ultrasonic activation of MNPs in such AMF in living systems is not practical.

4.2. Drug release remotely actuated by an AMF

A number of studies used magnetic heating to achieve controlled release of therapeutic agents from thermo-responsive drug carriers. Some of these studies observed effects that could not be explained by a purely thermic mechanism of activation.

Several studies used superparamagnetic MNPs embedded into or attached to lipid membranes of the so-called magnetoliposomes to disrupt these membranes by the

application of an AMF and thereby release a drug (or a probe that mimics a drug) encapsulated in the liposomes. Thus, Amstad et al. studied the release of calcein, a common fluorescent marker from the aqueous cavity of magneto-liposomes in which small MNPs of approximately 5 nm in diameter were hydrophobically coated with palmityl-nitroDOPA and incorporated in the lipid membrane [75]. The release was triggered by 5 min long AMF pulses (f = 230 kHz). Notably, the probe was released at a much lower temperature than the temperature at which the membrane phase transition would have occurred. A very similar study by Chen et al. used oleic acid coated 5 nm maghemite (Fe_2O_3) MNPs incorporated in membranes of 100 nm unilamelar liposomes [103]. This study demonstrated carboxyfluoresce-in release from the magnetoliposomes after their continuous exposure (2400 s) to an AMF ($B \sim 2.6$ mT; f = 281 kHz). In this case, the authors noted the bulk temperature increase of the sample due to the conductive heat transfer from the coil. However, this increase alone was not sufficient to alter the liposomal membrane permeability. Qiu and An examined release of calcein from 100 nm liposomes containing sodium bis(2-ethylhexyl)sulfosuccinate (AOT) coated magnetite MNPs [104]. Exposure of these liposomes for several minutes to an AMF of the sound frequency (no more data was provided in this paper about frequency, magnetic induction and gradient of the field) led to an accelerated release of calcein. Notably, the release of calcein at the same temperature upon bulk heating was several times slower than that produced by AMF activation. Therefore, the authors speculated that the permeability could increase due to both, moderate heating of the liposomes by the AMF and field-induced motions of the MNPs in the liposomal membranes that induced phase transition in these membranes and increased their permeability.

A very interesting study by Peiris et al. described the composite structures with chains of average 3 MNPs of 27 nm in diameter attached to 30 nm liposomes loaded with doxorubicin [105]. Exposure of these structures to the low frequency AMF (B = 0.5–2.5 mT, f = 10 kHz) led to drug release from the liposomes. No temperature increase was observed in this experiment, which was not surprising given low magnetic induction and field frequency. The authors explained the field-induced release of the drug by the mechanical disruption of the liposomal membrane caused by the motion of the MNP chains. Notably, this study demonstrated the AMF-induced death of the cancer cells pre-treated by these drug-containing structures as well as considerable antitumor effect in breast tumor-bearing rats treated intravenously with these structures 24 h before application of the magnetic field. In a more recent study by the same group this strategy was successfully used to demonstrate proof of concept for an improved method of glioblastoma treatment [106].

In a series of papers by Nappini et al. the release of fluorescent probes (carboxyfluorescein or Alexa 488-C5) from the magnetic liposomes was accelerated by exposure of these liposomes to the sound frequency AMF (B up to ~300 mT; f from 0.2 to 6 kHz, gradient up to 10 T/m) [107–109]. The authors prepared either large unilamellar liposomes (LUVs) ~160 to 200 nm in diameter or giant unilamellar vesicles (GUVs) ~5 to 50 μm in diameter, both incorporating cobalt ferrite ($CoFe_2O_4$) MNPs. The MNPs were ~10 to 16 nm in diameter and, depending on the surface coating, were incorporated either in the inner aqueous pool of the liposomes (negatively or positively charged MNPs) or in the lipid membrane (MNPs coated with a hydrophobic oleic acid shell) [107–109]. The concentration

of MNPs varied from 0.2 to 30 particles per liposomes. The exposure of these magnetic liposomes to the low frequency AMF resulted in the release of the probe, which increased as the frequency of the field, exposure time, or diameter and concentration of the MNPs increased. The authors explained their results by the formation of local pores or defects in the membrane, or some other structural changes of the bilayer that contributed to the permeability increase. Notably, in order to reduce the heating contribution of the MNPs in the AMF they have deliberately selected field frequencies several orders of magnitude lower than those needed for the magnetic hyperthermia. Yet the field amplitude was several times higher than in most hyperthermia studies, and thereby the heating component could not have been excluded. The experiment was carried in thermostatic cells at 25 ± 0.1 °C. However, the temperature may have increased not only due to the AMF but also the heating of the magnetic inducer as the setup did not appear to include its cooling. Overall, the observed effects were explained by a combination of hyperthermic effects and nanoparticle oscillations in the vesicles pool.

In addition to the liposomes a number of other nanomaterials with embedded MNPs have been proposed for controlled release. For example, Banchelli et al. immobilized thiolated oligonucleotides (10- and 18-mer) on cobalt ferrite MNPs with a gold shell (diameter 20 nm, diameter of $CoFe_2O_4$ core ~12 nm), and then cross-linked the resulting DNA-functionalized MNPs by hybridization with half-complementary DNA sequences [110]. The hybridization resulted in the self-assembly of the MNP–DNA clusters. Upon treatment of the clusters with the low frequency AMF ($f = 6$ kHz) over several minutes a considerable portion of the double strand DNA (up to ~40%) dissociated and released a single-strand DNA. Interestingly some small amount of double strand DNA was also released suggesting cleavage of the double strands from the gold surface during the treatment. The melting temperature of the double strands, which ranges from 50.8 to 53.5 °C and, based on our own estimates of the SAR by MNPs for this system, was most likely not achieved during the experiment (although data on temperature was presented). However, the authors concluded that the main reason of the observed effect is the DNA melting due to the local increase of the temperature.

A recent study prepared micellar structures by blending an amphiphilic block copolymer, poly(N-isopropylacrylamide-*co*-acrylamide)-*block*-poly(ε-caprolactone) and magnetite MNPs, hydrophobically coated with oleylamine (11 nm in diameter). The resulting ~70 nm in diameter aggregates were loaded with doxorubicin. The "magnetic" heating of these aggregates to 45 °C using an AMF ($f = 330$ kHz) resulted in 3 times faster release of the drug than the bulk heating to the same temperature in a water bath [111].

Thomas et al. described an interesting nanomaterial using mesoporous silica nanoparticles (MSNs) with zinc-doped iron oxide nanocrystals impregnated within a mesoporous silica framework [112]. The MSNs with a mean hydrodynamic diameter ranging from ~200 nm to ~300 nm were obtained by polymerization of silica precursor, tetraethylorthosilicate, on the cetyltrimethylammonium bromide (CTAB)-stabilized nanocrystals (15 nm). The MSNs were loaded with a concentrated probe (rhodamine B) or drug (doxorubicin) solutions and then sealed with cucurbit[6]uril to contain the solutes within the MSNs silica pores. The solutes were released from the MSNs by either bulk heating or local internal heating generated by

the nanocrystals upon exposure to an AMF (f = 500 kHz, amplitude 37.4 kA/m). After breast cancer cells (MDA-MB-231) were treated with doxorubicin-loaded particles and exposed to the AMF cell death occurred. To exclude the effect of the bulk heating on the drug release some experiments were carried out at 0 °C, which did not impede the field-induced release of nearly 90% of the entrapped solute. The authors interpreted their observations in terms of local internal heating, but it is interesting that the greater release was observed when the AMF was supplied in pulses rather that continuously, which, as discussed below, could not be entirely explained by local heating.

In some cases the MNPs are not incorporated within the thermosensitive nanoparticles but rather blended with them forming a composite material with remotely controlled drug release characteristics. For example, Langer and co-workers described a drug delivery device based on nanocomposite membrane containing thermoresponsive nanogels and superparamagnetic MNPs that can provide reversible, on–off drug release upon application (and removal) of an AMF [113,114]. The membrane consisted of ethyl cellulose membrane support, the superparamagnetic magnetite nanoparticles (10–20 nm), and thermosensitive poly(N-isopropylacrylamide) (PNIPAM)-based nanogels. The nanogels were relatively large and in aqueous dispersion underwent size change from about 700 nm to about 350 nm upon temperature increase from 37 °C to 50 °C. The magnetic heating of the membrane was induced by its exposure to an AMF (B up to ~20 mT; f = 220–260 kHz), which resulted in the collapse of the membrane impregnated nanogels and the increase of the membrane permeability with respect to both low molecular mass compounds and macromolecules.

In another study Štěpánek and colleagues co-incorporated thermosensitive liposomes of approximately 100 nm in diameter, preloaded with a fluorescent dye, and 15 nm iron oxide MNPs within microgel beads using the inkjet technique [115]. The size of the microgel beads ranged between 40 and 80 μm and therefore every bead contained multiple liposomes and MNPs. Upon exposure of these beads to an RF AMF (B = 20 mT; f = 400 kHz) the MNPs within the beads generated heat and the liposomes released the dye on demand. Interestingly, this experiment shows the limitations of the magnetic hyperthermia approach for the drug release purposes. No release was observed after the application of the AMF starting from the base temperature of 25° or even 37 °C when the concentration of the beads in the solution was 1%. Since the release for the liposomes could only start at approximately 40–45 °C, these temperatures could not be reached by AMF heating for the diluted system due to rapid heat dissipation to the environment. In order to reliably exceed the phase transition temperature of the lipid bilayer, a concentration of at least 25% has to be used. Obviously, such concentration may not be achievable in many delivery situations in the body, which demonstrates the limitations of the "pure" magnetic hyperthermia.

4.3. Magneto-mechanical stimulation of cells by an AMF

In order to reduce the heating contribution of the MNPs in the AMF to negligible levels and increase the mechanical component, some groups have deliberately selected field frequencies that are several orders of magnitude lower than those needed for the magnetic hyperthermia. Under conditions of a low-frequency AMF at $B \ll 1$ T and $f < 100$ Hz both local and bulk heating of cells and tissues can be neglected at any possible concentration of

the MNPs. In this case, however, the field can actuate mechanical motion of the MNPs, which in turn can affect the cells, subcellular structures and biomacromolecules to which such MNPs are attached. In brief, the results of the studies of such magneto-mechanical phenomena are summarized in this and following sections.

In particular A. J. El Haj and J. Dobson have engineered a special magnetic bioreactor in which AMF with an amplitude of up to 120 mT, gradient 11 T/m and frequencies from 0 to 1 Hz can be generated by the mechanically moved set of permanent magnets [116,117]. All experiments by these investigators described below were carried out using this bioreactor.

In one study Fe_3O_4 or CrO_2 micro- and nanoparticles ranging from 250 nm to 2.7 μm in diameter, were modified with either anti-His antibodies or complexes of nickel and nitrolotriacetic acid (Ni–NTA) (similar to those used in the purification of His-tagged proteins) to "target" the 6 histidine (6-His) loop regions of the recombinant protein ion channels TREC-1 [118]. TREC-1, a member of the 'background leak' family of tandem pore potassium channels (2PKC) highly expressed in various cells, is a true mechano-sensitive channel that also shows sensitivity to a diverse range of other stimuli including temperature, cellular lipids, free fatty acids, intracellular pH, G-protein-linked receptors and second messenger systems. The study demonstrated that manipulation with particles bound to TREK-1 resulted in activation of the channel activity in 6.His.loop.TREK-1 transfected COS-7 cells suggesting increased conduction of K^+ ions. These responses to magnetic particle stimulation were typically transient, lasting 2–10 s, which as the authors suggested was probably due to a desensitization of the TREK-1 channels to the mechanical stimulation or an adaptation of the cells to the applied stimulus. Notably, there was no obvious difference in the nature of responses following static or 1 Hz MNP stimulation which could suggest that the desensitization of TREK-1 channels to the initial stimulus failed to recover in time to show subsequent responses. Responses were absent when particles were coated with RGD (Arg-Gly-Asp) peptide that does not bind to TREK-1 or when magnetic fields were applied in the absence of magnetic particles. The observed phenomenon appeared to be similar to that of the "magnetic tweezers" with even the smallest of the nanoparticles affecting the individual ion channels. The estimate of the force generated by the MNPs as a result of the effect of the gradient field varied from 0.2 pN for the smallest (250 nm) to 40 pN for the largest (2.7 μm) particles [118]. Subsequent work applied magneto-mechanical stimulation to human bone marrow stromal cells (hBMSC) labeled with 250 nm magnetic beads targeting TREK-1 [119]. In this case the cells were stimulated with an AMF for 1 h each alternate day at cyclic loading intervals (f = 1 Hz, 1–100 pN/particle). Repeated stimulations resulted in enhanced proteoglycan and collagen synthesis, extracellular matrix production and elevated the expression of type-1 and type-2 collagen *in vitro* and *in vivo* (with cells encapsulated into polysaccharide alginate/chitosan microcapsules and implanted subcutaneously in mice).

In another study, this group demonstrated magneto-mechanical actuation of human osteoblasts cells using magnetic microparticles (4.5 μm) that were either integrin attached or internalized in the cells [120]. In this case the cells responded to the application of a static magnetic field (~56 mT; gradient ~4.0 mT/mm) by changes in the intracellular calcium signaling as was monitored by measuring the intracellular Ca^{2+} concentration. Interestingly,

the responses were greater when the magnetic microparticles were internalized in the cells rather than attached to the cell surface. Subsequently, the same authors applied magneto-mechanical stimulation in a tissue engineering application to induce differentiation of stem cells and bone formation [121]. This study used 250 nm MNPs modified with antibody to cell membrane receptors, platelet-derived growth factor receptor α (PDGFRα) or integrin αvβ3. The magneto-mechanical stimulation of PDGFR by the application of a static magnetic field (60 to 120 mT, gradient ~3.3 to 11.0 mT/mm) 1 h daily in the vicinity of the cells after 3 weeks increased the mineral-to-matrix ratio compared to stimulation of integrin αvβ3 and non-treated controls. The kinetics of osteogenesis and mineralization depended on the temporal schedule of the application of the magnetic field, which suggested the possibility to remotely control the tissue growth in the magnetic bioreactor. This was further demonstrated using functionalized MNPs (250 nm) to promote hBMSC differentiation towards a smooth muscle cell lineage by cyclical magneto-mechanical stimulation of PDGFRα and β *via* exposure to a magnetic field over a 3 h period at 1 Hz [122]. Overall these works provided proof of concept for remote controlled, locally-delivered mechanically-induced differentiation of hBMSCs which could have applications in regenerative medicine.

Results and prospects of magneto-mechanical activation of cell membranes are summarized in several other reviews that suggest that by properly choosing and modifying the MNPs one can selectively manipulate all mechano-sensitive structures of the cells including integrins, the cytoskeleton, kinase-type enzymes, mechano-sensitive enzymes (bound to the membrane and cytoskeleton) and mechano-sensitive ion channels (*via* membrane deformation) [31,123,124]. The future development of the magneto-mechanical stimulation of cellular functions and application of the emerging approaches in nanomedicine and nanobiotechnology requires engineering of small (~10 to 100 nm) MNPs with appropriate coatings that are stable in biological milieu *in vitro* and *in vivo* (in the presence of serum proteins and other biological components) and can react with individual molecules or supramolecular structures critical for cell function. One preview of opportunities and capabilities in this direction is provided by the study of the D. E. Ingber group [125]. They used superparamagnetic MNPs (~30 nm) that were modified with dinitrophenyl to selectively affect the transmembrane receptors that are normally activated by the binding of multivalent chemical ligands. These MNPs were pre-incubated with mast cells with IgE directed against dinitrophenyl so that the MNPs would bind to Fc1RI receptors on the cell surface through the antibodies. Activation of intracellular calcium signaling in response to the AMF was measured on single mast cells. A ferromagnetic needle of 10 μm was placed at a distance of 30 μm from the cell surface to serve as the field source. The field was induced by periodic (~1 min) switching on and off of the electric current, which led to a periodic increase in the intracellular concentration of calcium ions (Ca++) manipulated by the field. Due to the high field gradient (estimated ~10^4 T/m) the MNPs aggregated at the surface of the membrane, thereby causing clustering of the receptors and stimulation of the Ca++ signaling. This seminal work demonstrates possibility of activating individual cell membrane receptors through clustering, which acts as a nanomagnetic cellular switch that directly transduces magnetic inputs into physiological cellular outputs with rapid system responsiveness and non-invasive dynamic control [125].

4.4. Magneto-mechanical destruction of cancer cells and drug release by an AMF

In a bold departure from classic magnetic hyperthermia the authors of a series of papers proposed a purely mechanical approach for killing cancer cells that employed unusual magnetic properties of iron–nickel magnetic disks as vortices for cancer cell destruction [32,126–130]. These disks (~60-nm thick, ~1 μm diameter) were made of permalloy (80:20% nickel–iron magnetic alloy) and were coated with a 5-nm thick layer of gold on each side [127]. They were obtained by optical lithography and by magnetron sputtering to deposit gold layers. The disks had essentially no magnetization in the absence of magnetic field (zero remanent magnetization) due to spin vortex formation, and exhibited intrinsic spin resonance at low frequencies. After application of a super-low frequency AMF (f = 10–100 Hz, B up to 130 mT) the center of the magnetization vortex shifted vs. the geometric center of the disk, which resulted in the appearance of the macroscopic magnetic moment and led to the disk rotation in the field. In one of the studies the disks were coupled with anti-human-IL13α2R antibody that targeted the disks to the IL13α2R overexpressed on the surface of glioma cells [32]. As a result upon incubation of the disks with the glioblastoma multiforme cells the disks bound to these cells and then, after application of the AMF started rotating and killed the cells. Interestingly the greatest cell death was observed at an AMF with B = 10 mT and f = 10 to 20 Hz, while higher or lower values of B and f diminished the cell cytotoxic effect. The temperature of the cell culture was controlled and kept under 22 °C. Obviously, at such low field frequency no heating of the system by the AMF could be observed.

There is one example of the drug release induced by a magneto-mechanical effect that was accomplished using magnetic disk vortices already described above [126]. These disks were functionalized with chitosan and used as carriers for doxorubicin. Upon application of the AMF with f 10 Hz the drug was released from the disks with the release rate being proportional to the f. To expand the range of effective frequencies that trigger unloading of the drug the authors used two mutually perpendicular AMFs.

Although magnetic vortices represent an ingenious and promising approach, the current sizes of magnetic disk microparticles would hinder their use in many important nanomedicine applications. The particles of micron and even submicron size would be rapidly removed by the RES, would not extravasate in tissues and not cross biological barriers [131]. Therefore, the authors of this approach point out that to enable its use in nanomedicine the disk geometry can be scaled down to ~100 nm diameter while still preserving the spin-vortex properties [130]. The estimates of the magneto-mechanical effects that can be induced using magnetic microdiscs in an AMF are provided in the cited paper [128]. Although a decrease in the disk volume would decrease the total magnetic moment per disk and the magnetic torque, the torque can be recovered by increasing the magnetic field amplitude. For example a disk that is smaller in volume than the one described above (*e.g.* ~300 nm diameter, ~17 nm thin), will experience the same magnetic torque if subjected to a ~270 mT field, instead of the ~9 mT [128]. Stronger magnetic fields are possibly achievable since the required magnetic field frequency is only a few tens of Hz. However, as of today this approach has not been realized at the size scale required for the nanomedicine

and drug delivery applications (from 10 to 100 nm) and therefore still remains hypothetical for such applications.

4.5. Magneto-mechanical modulation of enzymes by a uniform AMF

Our studies have shown the possibility of a magneto-mechanical change of protein (enzyme) conformation and altering the rate of the biocatalytical reaction by an AMF in the absence of heating [33,132]. The effects of mechanical deformation on the functional properties of proteins and other bioactive molecules immobilized on polymeric supports have been studied for nearly 40 years [133,134]. Immobilization of an enzyme molecule on a polymer support followed by mechanical deformation of this support can result in deformation of the protein globule and considerable change of enzyme activity [135]. Such approaches can be further extended to single molecule studies to modulate biocatalysis, membrane transport, protein synthesis and other essential biological functions by mechanically affecting enzymes, membrane channels, ribosomes, etc. [136–139].

To explore the possibility of translating AMF exposure into change in the function of individual enzyme molecules we synthesized colloidal clusters by coating magnetite MNPs (7 to 12 nm diameter) with anionic poly(ethylene glycol)-b-polyacrylate or poly(ethylene glycol)-b-polymethacrylate block copolymers [33]. Each cluster contained up to 10–15 MNP cores electrostatically bound and cross-linked by the copolymers. The enzyme molecules, $e.g.$ α-chymotrypsin and β-galactosidase, were covalently coupled (through amino groups) to the polymer chains. The effects of the AMF were studied using two different setups. One was a regular RF AMF ($B = 26.4$ mT, $f = 337$ kHz) commonly used in magnetic hyperthermia. Another was a super-low frequency field (B up to 250 mT, $f = 10$ to 100 Hz) that was uniform ($i.e.$ zero gradient) within the entire sample volume in a striking contrast to most other studies described in this review that used gradient fields. The field uniformity ensured: a) same field conditions within the sample volume, and b) predominant effect of twisting moment upon MNPs with translational forces being negligible. In addition both the field space and the coil were well thermostated that ensured constant temperature during the experiment.

Exposure of the sample dispersion to both types of fields resulted in inactivation of the enzymes immobilized in the clusters [33]. Interestingly, the inactivation effect was the greatest when the fields were supplied in several pulses (2–3 min) rather than continuously for the same overall durations. Similar observations were also reported for an enzyme (α-chymotrypsin) immobilized on the ~30 nm nanoparticles with magnetite MNP cores and gold shell [132]. These studies provided very strong arguments in support of the non-thermic mechanism of enzyme inactivation. First, the experiments were carried out at 20 °C to 25 °C and changes in the bulk temperature were negligible. Second, measurements in the absence of the field suggested that comparable inactivation of enzymes immobilized on same MNPs only occurred at 45–50 °C. Third, no local heating effects could have taken place upon exposure to super low frequency fields ($f = 100$ Hz). Fourth, the inactivation effect increased as the number of the points of attachment of the enzyme to the polymer support increased, which is more consistent with the mechanical but not thermic mechanism of inactivation. Even effect of the pulses at high frequency of the field argued against a thermic mechanism

as the periods between the pulses (several minutes) facilitate heat dissipation in the environment. Finally, the circular dichroism (CD) showed that pulsed exposure to the AMF resulted in changes in the secondary structure of the immobilized enzyme that were very different from those observed upon heat denaturation of the same samples [33].

The observed phenomena were predicted and explained by theoretical analysis suggesting the possibility of translating the energy of a non-heating AMF (f < 1 kHz) to the mechanical deformation of macromolecules immobilized on MNPs [140–142]. Specifically, realignment of the MNPs along the AC magnetic field may lead to stresses in MNP-linked polymer chains. A chain attached to two particles in a MNP cluster can undergo tensile, compression, twisting and tangential (grinding) forces actuated by an external AMF (Fig. 5). A MNP experiences torque L, which leads to its rotary-oscillating movement. In turn the macromolecule attached to MNPs can undergo tensile, compression, twisting and shear deformation (depending of the mutual orientation of the magnetic moments μ_i of oscillating MNPs, direction of the vector of magnetic induction B and the points of attachment of this macromolecule to the MNPs). The estimates of forces F that could act upon the macromolecule chain attached to two MNPs are presented in [140–142]. These estimates suggest that upon exposure of MNPs to B < 1 T, the resultant F could be as high as hundreds of pN and cause deformations up to dozens of nm. As found from Single Molecule Force Spectroscopy studies such forces and deformations are sufficient to induce various macromolecular transitions and stimulate some processes that are essential for nanomedicine and drug delivery (Table 1) [38,143–146]. Therefore, a variety of applications in nanomedicine and drug delivery can be explored using readily achievable magnetic fields with B from a few dozen to a few hundred mT.

4.6. Magneto-mechanical cell injury by MNPs in a rotating magnetic field

Some studies used a rotating or precessing magnetic field with the rotation axis of the induction vector being perpendicular or tilted in relation to the direction of the field instead of an AMF. The amplitude of such field could be either constant or altering with a given frequency. In essence, a rotating field is a kind of an AMF. It is usually produced by a reciprocating or rotary movement of constant magnets or superposition of two orthogonal AMFs having a phase shift π / 2 between each other. Mizuki et al. studied the effects of a rotating magnetic field on superparamagnetic magnetite MNPs coated with dextrane (~130 nm in diameter) and containing immobilized enzyme (α-amylase) [147]. The particles assembled into clusters of ~1000 particles that rotated with the field with a frequency of 1 Hz. Once the frequency increased the clusters broke down to smaller ones containing few hundred of particles, and then further broke down to individual particles as the frequency exceeded 5 Hz. Concurrently, the activity of the enzyme increased as the field rotation frequency increased reaching a maximum at 5 Hz and then decreased again at higher frequencies. They explained this phenomenon by the increased collisions of the substrate and enzyme molecules in the rapidly rotating clusters but, unfortunately, the paper did not provide sufficient experimental detail to determine the mechanism. In our opinion the activity change could occur due to the shift from a diffusion controlled to a kinetically controlled regime of enzyme reaction due to better mixing at 5 Hz followed by inactivation of the enzyme by the shear stress at higher frequencies.

In a more recent study Zhang et al. used commercial superparamagnetic MNPs (~100 nm) to induce cancer cell death by the rotating magnetic field [148]. The MNPs were modified with antibody against lysosomal membrane protein, LAMP1, to enhance their binding with the lysosomal membranes. Remote activation of the slow rotation of LAMP1-modified MNPs by the magnetic field (B = 30 mT) rotating at 20 Hz enhanced the MNP uptake in the cells where they were preferentially localized in the lysosomal membranes due to binding with LAMP1. Subsequent exposure to the rotating field resulted in lysosome injury and death of the cancer cells. The authors underscore that in contrast to the reports using high-frequency alternating (but not dynamic) magnetic fields their approach uses a low-frequency rotating field that induces the rotation of every individual particle in the field around their own axis and thereby causes apoptosis *via* mechanical forces exerted on membranes by targeted MNPs without any heating [85,149].

5. Models of the magneto-mechanical effects of an AMF

The studies discussed above observed the cell injury, drug release, enzyme inactivation and other non-thermic effects of the low frequency and super-low frequency AMFs translated to biological systems by MNPs. Some of these effects appeared to depend on the parameters of the field. However, no detailed theory or quantitative model of such effects has been developed so far. Such theory could be highly instrumental for the rational design of MNPs including selection of proper sizes and structures, as well optimization of the field parameters, that would best suit the desired pharmacological effect of such MNPs in an AMF. Previously, we have published theoretical analyses pertaining to select magneto-mechanical phenomena such as macromolecule or membrane deformation by the low-frequency AMF [140–142,150,151]. This chapter presents a systematic consideration and extension of several quantitative models that could serve purposes in nanomedicine and drug delivery as well as other biomedical and bioengineering applications.

5.1. Dynamics of MNPs in an AMF

Let us consider a case of a core–shell nanoparticle with a MNP core and a solid (*e.g.* gold) shell that can be grafted with polymer chains forming a corona (Fig. 3). The therapeutic agent can be attached to this polymeric corona either covalently or through various non-covalent interactions. The behavior of such functionalized MNPs after exposure to a uniform AMF will depend on the ratio of their magnetic energy in the field vs. losses of energy to viscous friction as well as the magnetostatic interactions and energy of thermal vibrations [151]. One can neglect the magnetostatic energy of interactions of MNPs if these particles have a gold and/or polymer coatings with the net thickness exceeding several times the radius of the magnetic core R_m. The contribution of the thermal fluctuations will be discussed below.

It is well known that the energy of the system reaches its minimum when the vectors **μ** and **B** become collinear and co-directed. Let us further assume that upon change of the instant value of the field B according to a sinusoidal law with the frequency f the relaxation of the magnetic moment of the MNPs proceeds *via* the particles' mechanical rotation, *i.e.* the Brown relaxation (Fig. 4). A competing process is the Neel relaxation, when the MNPs

remain immobile, but the spins of each atom of ferromagnetic rotate overcoming the energy of crystallographic anisotropy. Brown relaxation proceeds faster than Neel relaxation, if the radius of MNPs is greater than some critical value R_c (see Supplementing material 1). This value depends upon the nature of a ferro- or ferrimagnetic material. For example, for magnetite (one of the most frequently used materials for preparation of MNPs) this value $R_c \approx 7$ nm [24]. Therefore, to ensure efficient transduction of the AMF energy to the energy of the MNPs' mechanical movement the MNPs should have a radius $R_m > R_c$. However, at a low frequency of an AMF (when the half-period of field oscillation exceeds the Brown relaxation time) the small MNPs that first respond by Neel relaxation can also follow up by the mechanical spinning. Under these conditions the angle between the direction of the field vector and axis of the small spontaneous magnetization decreases, which contributes to the decrease of the magnetic energy of the system.

Taking into account the above assumptions the rotational movement of a free spherical MNP in a viscous media exposed to the AMF is described by the following equation:

$$I\ddot{\varphi} = \mu \mathrm{B} \sin\omega t \sin\varphi - 6\eta V_{HD}\, \dot{\varphi}, \quad (1)$$

where φ – is the angle between the vector of the magnetic moment of the MNP and direction of the AMF in even half-periods, ω – is the cyclic frequency of an AMF $\omega = 2\pi f$, I – is the moment of inertia of MNP, and V_{HD} – is the hydrodynamic volume of the MNP. The characteristic frequency ω_I, *i.e.* the frequency above which the inertia of the MNPs cannot be neglected, is determined from the following equation $I\omega_I^2 = \mu \mathrm{B}$. For the magnetite MNPs with the radius of the nuclear core $R_m \approx 10$ nm, having a gold shell of 5–8 nm and hydrodynamic radius $R_{HD} \approx 30$ nm in the field $B \approx 0.1$ T the characteristic value $\omega_I \approx 10^7$ s^{-1}. If $\omega \ll \omega_I$

Eq. (1) can be presented as follows:

$$\omega_c \cdot \sin\omega t \sin\varphi = d\varphi/dt, \quad (2)$$

where the critical frequency parameter $\omega_c = \mu \mathrm{B}/(6\eta V_{HD})$. Because magnetic moment μ of a single domain magnetite nanoparticle is the product of magnetite saturation magnetization J_s and its mass, which in turn is the product of magnetite density ρ and volume V_M, critical frequency can be expressed as $\omega_c = B \dfrac{J_s \rho}{6\eta} \left(\dfrac{R_M}{R_{HD}} \right)^3$, where R_M is the magnetite core radius. For MNPs having $R_M / R_{HD} = 1 / 2$ in an aqueous media or another media with the viscosity $\eta = 0.65 \cdot 10^{-3}$ Pa $\cdot$ s at 40 °C exposed to the field $B \approx 100$ mT this parameter $\omega_c \approx 1.5 \cdot 10^6$ s^{-1} ($f_c \approx 250$ kHz). This could be considered an estimate of the maximal ω_c parameter, as an increase in the hydrodynamic diameter of the MNPs (larger shell), lower field or higher viscosity should result in its significant reduction. For example, for MNPs with $R_M / R_{HD} = 1 / 5$ in the media with the viscosity that exceeds that of water by 1–2 orders of magnitude in 10 mT field the ω_c value becomes as low as ~10–100 s^{-1}. Thus, the critical frequency f_c lies in the range from a few hertz to several tens of kilohertz in most plausible cases.

The solution of Eq. (2) is as follows:

$$tg\frac{\varphi}{2} = tg\frac{\varphi_0}{2} \cdot \exp\left(\frac{\omega_c}{\omega}(1-\cos\omega t)\right). \quad (3)$$

According to this solution the MNPs are moving periodically returning after the entire period to their initial state with an angle φ_0. However, in reality upon transition of the field through the zero value during time $\tau \approx 2k_B T/(\omega\mu B)$ the particle will be subjected to heat oscillations that will result in the uncertainty of its angular position $\varphi^2 = k_B T\tau/(6\eta V_{HD})$. At $\omega \approx 10^3$ s^{-1} for the MNPs discussed above $\tau \approx 10^{-6}$ s, hence the mean deviation is $\langle\varphi^2\rangle^{1/2} \approx$ 0.1 rad. After several periods of AMF oscillation this will lead to a symmetric rotational–vibrational movement of MNPs relative to the direction of the field. Then the following conclusions can be made from the equation of the steady movement, symmetrical relative to position $\varphi = \pi/2$,

$$tg\frac{\varphi}{2} = \exp\left(-\frac{\omega_c}{\omega}\cos\omega t\right). \quad (4)$$

At $\omega \ll \omega_c$ MNPs undergo sharp flip-flop like turns after each change of the sign of the external AMF (Fig. 5). As the frequency ω increases the role of viscosity increases and under the condition $\omega \gg \omega_c$ the oscillations should asymptotically approach a harmonic with small amplitude: $\varphi = \pi/2 - (\omega_c/\omega)\cos\omega t$.

Based on the dependence of the amplitude of oscillation of MNP φ on the frequency $\varphi = 4\arctan[\exp(\omega_c/\omega)] - \pi$ (Fig. 6, curve 1) one can conclude that at $\omega \ll \omega_c$ $\varphi \approx \pi$, and at $\omega \gg \omega_c$ φ approaches zero. The fraction of time during which the MNP moves with an angular velocity close to ω_c, depends on φ according to the equation $t/t^\propto \varphi \cdot (\omega/\omega_c)$ (Fig. 6, curve 3).

The hydrodynamic force F_{HD}, acting upon the therapeutic molecule R_{mol} attached to the shell of the MNP can be determined using the Stokes equation:

$$F_{HD} = 6\pi\eta R_{mol} \cdot v = 6\pi\eta R_{mol} R_{HD} \cdot \dot\varphi. \quad (5)$$

The value of this force is proportional to the instant angular velocity $\dot\varphi(t)$ that is presented in Fig. 5b. As follows from Eq. (2), $|\dot\varphi(t)| \leq \omega_c$, so that maximal possible value of F_{HD} is $F_{HD\max} = F_{HD}(\omega_c)$ and relative hydrodynamic force $\frac{F_{HD}}{F_{HD\max}} = \frac{|\dot\varphi_{\max}|}{\omega_c}$. At condition $\omega \gg \omega_c$ the maximal value of the angular velocity $|\dot\varphi_{\max}| = \omega_c$, and at $\omega \ll \omega_c$ its value $|\dot\varphi_{\max}|^\propto (\omega\omega_c)^{1/2}$. So, at $\omega \gtrsim \omega_c$ amplitude value F_{HD} depends neither on ω nor on η and approaches $F_{HD\max}$, but at $\omega \ll \omega_c$ this value $F_{HD}^\propto \omega^{1/2} \cdot \eta^{1/2}$. (Fig. 6, curve 2). For a therapeutic agent molecule having a radius $R_{mol} = 2.5$ nm, attached to MNP having the above considered parameters in the viscous media with $\eta \approx 10^{-3}$ Pa · s, the amplitude value $F_{HD} \approx 0.1$ pN.

5.2. Hydrodynamic models of release of therapeutic agent from MNPs

Here we consider possible mechanisms of release of a therapeutic agent from the polymeric corona of MNPs induced as a result of the action of AMF. We assume that the therapeutic agent is bound with the polymeric corona with one or few number of bonds (*i.e.* the cooperativity of interaction is zero or relatively low). This assumption is likely to be correct for relatively low molecular mass therapeutic agent molecules. We also do not consider possible entropic contributions of the polymer chains and therapeutic agents as well as contributions of low molecular mass counterions that could play a significant role for polyelectrolytes.

In thereby simplified consideration, the potential energy U_b of interaction of the therapeutic agent with the polymer chains in the corona of the MNPs should be sufficiently high to avoid a spontaneous release from the particle as a result of the heat oscillations, random collisions of MNPs with each other, etc. At the same time the U_b value should not be too high to ensure that the rotary-oscillating movement of MNPs upon exposure to AMF led to an accelerated release of the therapeutic agent. It is reasonable to consider the van der Waals, electrostatic and hydrogen bond interactions between the therapeutic agent and MNP polymeric shell. The covalent bonds are too strong to be cleaved using AMFs that are readily accessible in the laboratory (Table 1). The energy profile of the van der Waals interactions (Fig. 7, curve 1) is assumed to be more flat than the profiles corresponding to electrostatic interaction and/or hydrogen bond interactions. The van der Waals interactions profile has random perturbations due to local interactions of the neighboring therapeutic agent molecules, polymer chain local curvature, etc. The small minima could be found due to localization of the therapeutic agent on the polymeric chain. In the cases of electrostatic interaction and/or hydrogen bond interactions the energy profiles will also have minima, which could be deeper and more regular (Fig. 7, curve 2). Both curves are limited at the left side by an infinitely high barrier due to the presence of the MNP "wall", and at the right side with a finite barrier which corresponds to the detachment of the therapeutic agent from the polymer chain. With these assumptions two release mechanisms are briefly summarized below (their more detailed consideration is provided in the Supplementary material 3).

The first mechanism is based upon hydrodynamic force acting on the therapeutic agent molecule due to the rotational–vibrational movement of MNPs in the external AMF. The overall energy profile is tilted to the left because of the affect of the hydrodynamic force F_{HD} acting upon the therapeutic agent molecule. It should be noted that the slope of the profile is always negative starting from the MNP surface, although its magnitude is changing over time as the AMF oscillates. As the therapeutic molecule agent undergoes thermo-activated random walk along the chain the affect of this weak hydrodynamic force imposes a drift of this molecule towards the outward end of the polymer chain that accelerates the therapeutic agent release.

The second mechanism considers the therapeutic agent molecules bound to two polymer chains simultaneously. If the chains are stiff enough, MNP rotational–vibrational movement results in an oscillating force applied through the chains to the therapeutic agent molecule bound between them. This force facilitates overcoming the barriers between neighboring energy minimum positions that effectively accelerates the movement of the therapeutic agent

along the pair of polymer chains in any direction. The effect is small at the beginning because initially the number of therapeutic agents interconnecting the polymer chains is high and the forces are divided between them. But as some part of therapeutic agent molecules are released, the second mechanism can noticeably accelerate the release of the remaining therapeutic agent molecules.

5.3. Models of interaction of a rod-like MNP with a lipid membrane

The model of the therapeutic agent release described above accounts for relatively weak hydrodynamic forces created by the movement of functionalized MNPs in viscous media. The magnitude of the magneto-mechanical effects could greatly increase if the torque L of the MNP in the AMF is balanced by the forces of contact interaction of MNPs with supramolecular structures, such as elements of biological membranes, liposomes, micelles, etc. In this case the rotational–vibrational movement of MNPs can cause deformations and structural transitions that can translate into functional changes remotely induced by the AMF. A recent study by Golovin et al. considered a model of interaction of rod-like MNPs with a lipid membrane [150]. Anisometric MNPs have several advantages in terms of magneto-mechanical actuations compared to spherical MNPs. In particular, in addition to the shear they can also cause normal deformations in the membrane. A general case is presented in Fig. 8. A rod-like MNP with the length L_M and midsection diameter D having magnetic moment $\boldsymbol{\mu}$ is attracted to the bilayer lipid membrane by the relatively weak adhesion forces (van der Waals, dispersion and hydrogen bond). In most cases there are also the forces of electrostatic attraction as many MNPs are either conjugated with polyelectrolytes or carry excessive surface charge. In the case of a live cell and MNPs functionalized by antibodies or other ligands the MNP is strongly attached *via* these ligands to the cell receptors, ion channels and other structural and functional components of the biological membrane.

Application of the AMF having arbitrary orientation of the induction vector $\boldsymbol{B}$ induces a complex oscillating movement of MNP reminiscent of the movement of the double paddle of an Aleutian kayak. This is accompanied with the appearance of oscillating forces and deformations with the oscillating and lateral components (Fig. 9). Assuming that the force is concentrated at the ends of the MNP the estimate for the maximal value of its normal component is as follows:

$$F_z \approx J_s \rho_M V_M B_z / L_M, \quad (6)$$

where J_s – is saturation magnetization, and ρ_M and V_M – are the density and volume of the MNP, respectively. Since $V_M \approx D^2 L_M$, the value of F_z as first approximation does not depend on L_M. Therefore, $F_z \approx 150$ pN for the rod-like magnetite MNPs having $D = 30$ nm, placed in a field with $B_z = 0.5$ T. The mechanical deformation of the membrane caused by the force F_z is mainly dependent on the mechanical rigidity E^* of the membrane (and in the case of the cell also by the rigidity of the cytoskeleton), where $E^* = 0.1–10$ kPa [145]. Already in a field with $B = 0.1$ T the local pressure $P \approx F_z/D^2 \approx 40$ kPa near the ends of the MNP exceeds E^* several fold which may lead to the rupture of the membrane. In the case of the cell membrane this could result in the death of the cell (*e.g.* cancer cell).

Let us now consider the movement of the MNP in the plane of the membrane (Fig. 9). As the oscillating field B increases after passing zero and the MNP long axis and magnetization vector μ orient along the projection of B to the membrane surface at an angle ϕ_0, the MNP starts to rotate to achieve co-linearity of μ and B. In a general case this movement will be described by an equation similar to Eq. (1) describing the dynamics of the movement of a spherical MNP. In this case, however, the parameter η has a meaning of a characteristic viscosity that is determined by the force of viscous resistance of the surrounding (membrane, structures). At $\omega \ll \omega_I \approx 10^7 \ \mathrm{s}^{-1}$ Eq. (1) transforms to Eq. (2), and its solution to Eq. (3).

The angle swept that is passed by the MNP is $\phi = 2\mathrm{arc}\,tg[tg(\phi_0/2)\exp(2\omega_c/\omega)] - \phi_0$. The maximal value of ϕ depends on ω similar to the curve 1 in Fig. 6. This means that the considered magneto-mechanical effects can take place only at the AMF frequencies $\omega < \omega_c$. The effective viscosity upon interaction of the MNP with the membrane can be much higher than that in the aqueous solution; the estimates of ω_c for magnetite MNP with $D = 10$–20 nm and aspect ratio $L_M/D \approx 5$–10 at $\eta \approx 0.1 \ \mathrm{Pa} \cdot \mathrm{s}$ range from 100 to 1000 s^{-1}.

Upon considering the 3-D movement of the MNP, one should account for the moment of inertia that in general is not a scalar quantity but a tensor of the second order. Therefore, the pressure upon the membrane grows concurrently with the rotation of the MNP. As the field induction passes zero the normal and lateral projections of the field change the sign. If $\omega \ll \omega_c$, the orientation of MNP will flip-flop by 180° followed by an increase of the normal tensions of the membrane near the ends of the MNP. The direction of the deformation will remain the same.

The rotation of the MNP in the plane of the membrane creates wave-like shear deformations in the circle of diameter $\sim L_M$. The amplitude of these deformations can also be sufficient for the destruction of the membrane because the value of $4F_x/L_M$ in the field $B = 0.1$ T is comparable with the linear tension of the membrane $\sigma \approx 0.01 \ \mathrm{N/m}$ [145]. Similar considerations are also correct for the MNPs embedded in the membrane structure (at any angle to the membrane plane). The combined action of normal and lateral tensions and deformations, comparable with the energies of interaction of the molecules in the membrane (including biomacromolecules embedded in the membrane) can be achieved in the low frequency AMF with induction much less than 1T. This can cause the loosening of the membrane and increase in its permeability long before its physical destruction. In the conditions when $\omega \gg \omega_c$, the MNP may remain nearly immobile, but the membrane may experience the sign alternating deformations near the ends of the MNP.

If in addition to the dispersed adhesion forces the MNPs are connected to the membrane covalently *via* strong ligand–receptor bonds (Fig. 8) the estimated value of the lateral force F_{MM} determined using an equation similar to Eq. (6) can be as high as $F_{MM} \approx 300$ pN (assuming that there are two strong attachment points). If the MNP is strongly attached to the membrane not on its tips but closer to its center the F_{MM} value can increase even further several fold. Taking into account the data on the forces characterizing various molecular interactions in biological membranes and cells and using Eq. (6), one can estimate the required values of the field B to induce magneto-mechanical affects that disrupt these

interactions which in many cases are in the range of dozens to hundreds of mT (Table 1). The presented model can be also useful for understanding of the effects of very small (*e.g.* 5 to 10 nm) MNPs, that, in certain conditions, interacting with each other and the membrane can assemble into 2D rafts or rods and behave similar to rod-like MNPs described in this section [141].

The choice of an optimal AMF frequency range for the magneto-mechanical stimulation of the membrane receptors is complex and requires a separate consideration and investigation. Different molecular structures in the cells and the functional processes controlled by them are known to have different characteristic times ranging from nanoseconds to hundreds of seconds [152–154]. In essence, a cell can be considered a "frequency bandwidth filter" of sorts that is capable of responding to mechanical actuation of a specific frequency or duration [155]. This can have enormous consequences for nanomedicine because in addition to a commonly discussed spatial selectivity of nanomedicine technologies (realized through a precise delivery of the nanoparticles to certain receptors or structure in the target cell) one could employ the frequency selectivity that can be achieved by tuning the magneto-mechanochemical stimulation.

5.4. Model of magneto-mechanical deformation of biomacromolecules

As discussed above the forces acting on macromolecules attached to the single MNPs with a hydrodynamic radius $R_{HD} < 100$ nm, have a hydrodynamic nature and by the order of magnitude do not exceed 1 pN. Much greater forces can be observed in the aggregates containing two and more MNPs interconnected with each other by one or several macromolecules that are linked simultaneously to two or more MNPs. Such forces will have a contact nature. They can cause deformations of biomacromolecules that in the case of enzymes or receptors can change the conformations of the active centers and modulate functional activity of such biomacromolecules. The models of the magneto-mechanical deformation of enzymes were recently discussed in the literature [140–142]. Here we briefly summarize them.

In the simplest case of an aggregate – a dimer of MNPs interconnected through one macromolecule (Fig. 10) the movement of each MNP is described by the system of equations:

$$M\ddot{\boldsymbol{r}} = \boldsymbol{F_e} - 6\pi\eta R_{HD}\,\dot{\boldsymbol{r}} \quad (7)$$

$$I\ddot{\boldsymbol{\varphi}} = \boldsymbol{\mu} \times \boldsymbol{B} - \boldsymbol{F_e} \times \boldsymbol{R_{Au}} - 6\eta V_{HD}\ddot{\boldsymbol{\varphi}}, \quad (8)$$

where $\boldsymbol{F_e}$ – is the constraint reaction force, $\boldsymbol{r}$ – the radius vector of the particle center, and $\boldsymbol{R_{Au}}$ – radius vector from the center of MNP to the point of application of $\boldsymbol{F_e}$.

Analysis of Eqs. (7) and (8) suggest that for any reasonable length of the interconnecting chains, upon exposure to the external AMF the MNPs, are pulled by the constraint reaction forces and rapidly come in contact with each other. The time of their rapprochement t^* depends on the main parameters of the system as follows:

$$t^* \sim \sqrt{\frac{\eta \cdot R_{\mathrm{Au}} \cdot R_{HD} \cdot l_0}{\omega \cdot \mu \cdot B_a}}, \quad (9)$$

where l_0 – is the initial distance between MNPs, B_a - is an amplitude value of MF intensity. The value t^*, normalized by the period of oscillations of the external AMF ($T = 2\pi / \omega$) is proportional to $\omega^{1/2}$. At $\omega \sim 10^4$ s^{-1} one concludes that $t^* / T \sim 10^{-2}$. Because the rapprochement of the MNPs proceeds much faster than the external field period one can exclude from the consideration of Eq. (7) the translational movement of MNPs.

Since the long linkers due to their own deformation decrease the magneto-mechanical affect upon the macromolecules, it is advisable to use short linkers. In this case the net length of the linker and the polymer chains separating two MNPs in general becomes much less than the size of the MNP aggregates. In such systems the linking chain can be fixed in the points close to the axis connecting the centers of MNPs. Being affected by the AMF, the MNPs in "dimer" form are in contact with each other during the most part of the period, so the forces of deformation appear due to particle rotation in the AMF being constrained by the linker chain. Further, we consider exactly such "dimer" aggregates.

Upon exposure to the AMF such a system undergoes a complex oscillating motion, that is a sum of the motions of the dimer as a whole and the relative motions of each MNP within the dimer. During the first $\sim 10^{-6}$–10^{-5} s after exposure to the external field (that is a small fraction of the period in the range of frequencies of interest to us) the dimer "adjusts", to the changed conditions and then its vibrational movements become steady. These adjustments include two turns. The first one is the rotation of each MNP across the axis connecting the center of the MNPs, so that their magnetic moments $\boldsymbol{\mu_1}$ and $\boldsymbol{\mu_2}$ become coplanar with vector $\boldsymbol{B}$ and each other. The second one is the rotation of the dimer axis to ensure that the sum of the magnetic moments $\boldsymbol{\mu_1} + \boldsymbol{\mu_2}$ becomes collinear to $\boldsymbol{B}$.

In the phase of steady oscillations upon the increase of the external field the magnetic moments of the MNPs in the dimer are oriented symmetrically to the field lines, and the dimer net moment is codirectional with $\boldsymbol{B}$. The MNPs will rotate in different directions essentially rolling over each other's surface, trying to align their magnetic moments along the field lines, and the centers of MNPs will remain immobile. The interconnecting chains will stretch and counteract the rotation of the MNPs. As the field goes through zero and changes the sign to the opposite the net magnetic moment $\boldsymbol{\mu_1} + \boldsymbol{\mu_2}$ and the vector $\boldsymbol{B}$ will become oppositely directed, which will result in a flip-flop of the dimer to 180° relative to the axis, perpendicular to the field direction. The $\boldsymbol{\mu_1} + \boldsymbol{\mu_2}$ and $\boldsymbol{B}$ will become co-directed, and the movement, similar to that described above will repeat itself.

The movement of each MNP in the regime of steady oscillations is entirely described by Eq. (8). Assuming as first approximation the viscosity and inertia forces being negligible (at $\omega \ll \omega_c$ and $\omega \ll \omega_l$) the equation can be presented as follows:

$$2cR_{\mathrm{Au}}^2(1-\cos\varphi)\sin\varphi = \mu B_a \sin(\omega t)\sin(\theta-\varphi), \quad (10)$$

where $\theta-$ is the angle of initial orientation of the magnetic moments of MNPs relative to the field lines. The parameter c has a meaning of some effective value of the rigidity of macromolecule [143,144,146]. Accounting for the non-linearity of the deformation of macromolecules does not change in principle the character of the MNPs motions.

A direct consequence of Eq. (3) is that the dimensionless parameter $\lambda = \mu B_a / (2cR_{Au}^2)$ reflecting the ratio of the characteristic torques of magnetic interaction and the constraint reaction forces, entirely defines the motion of the MNPs if the initial orientation of vectors μ described by the angle θ_0 is known. One can suggest that at $\lambda \gg 1$ when the moment of the constraint reaction forces can be assumed negligible compared to the moment of the AMF forces each MNP behaves as an individual particle. The time of the active deformation of the macromolecule, in this case, can be several orders of magnitude lower that the period of oscillation of AMF. At $\lambda \ll 1$ the amplitude of oscillation of the MNPs will be very small. Typical values of the parameter λ for the magnetite MNPs with $R_m = 7$–10 nm, $\delta \sim 5$ nm, $c \sim$ 1–10 mN/m in AMF with induction $B_a \sim 0.1$–1 T range from ~0.1 to ~10. The possibilities to increase this value by increasing the sizes of the magnetic nuclei are limited because of the tendency of such particles to aggregate due to the increased dipole–dipole interactions. Creation of AMF with $B \gtrsim 1$ T is technically challenging. The parameter λ can be increased by selecting materials with greater J_s value (for example Fe, Co, Ni, their alloys, some lanthanides). However their biomedical applications is hindered by high toxicity.

As could be seen in Fig. 11 the dependencies of the maximal force F_{max} and deformation l_{max} on the main parameters (B_a, c, R_m) are monotonous. Non-monotonous under certain conditions is the dependence of l_{max} on the thickness of a shell δ, when there is an optimal value δ, that results in maximal deformation.

The statistics of the angles of the initial orientation of the magnetic moments of chaotically disoriented MNPs relative the vector B affects the mean value of the force. Accounting for the above assumption of free rotation of MNP around the axis of the dimer and assuming the uniform initial spatial angle distribution of the MNPs' magnetic moments its azimuthal angle is distributed as $p(\theta) = \cos\theta\,d\theta$. Therefore, the difference of the angles of orientation of MNPs in one plane is distributed as:

$$p(\Delta\theta) = [(\pi - |\Delta\theta|)\cos\Delta\theta - \sin|\Delta\theta|]/8, \ \Delta\theta \in [-\pi;\pi]. \quad (10)$$

The mean value $|\theta|$ is $\pi/4$, that corresponds to the mean angle of initial disorientation of the magnetic moments $\theta = \pi/8$.

In addition to macromolecules attached to the linkers that participate in the formation of bonds between MNPs, the mechanical stress can be also experienced by the macromolecules attached to the MNP surface when they become entrapped between the oscillating MNPs. Such macromolecules undergo different types of deformation like compression, twisting and shear. The macromolecules affected by these stresses are located in the arch-shaped region of contact of the MNPs having the length $R_{Au}\varphi_{max}$ and width $\sqrt{2Rd}$, where $d \sim 5$ nm is a characteristic diameter of the macromolecule. Based on this the fraction of the

macromolecules that undergo deformation (assuming their uniform distribution in the surface of the MNPs) can be estimated as $\varphi_{max}/4\pi \sqrt{2d/R_{\mathrm{Au}}}$. Its limiting value $1/8 \sqrt{2d/R_{\mathrm{Au}}}$ for typical MNP sizes in the considered model is ~10–15%. In the "real" conditions where there are more than two bonds with long linkers the fraction of macromolecules undergoing deformation can reach 20–30%. The statistics at given values of λ can be derived from θ distributions and the equation of motion discussed above.

The deformation force F_s at a small λ depends on the current angle of the MNP turn as follows $F_s = cR_{\mathrm{Au}}\varphi^2/2$. Its maximal value for particles with $R_m = 7$–10 nm, $\delta \sim 5$ nm, $c \sim 10$ mN/m in the AMF with $B_a \sim 0.5$ T is about 250 pN. The mean compression and shear stress in the macromolecule can be as high as ~100 MPa. Such forces and resulting strains, like in the case of the linear tension of the macromolecule are sufficient to significantly change its conformation.

In a real situation heterogeneity of the geometry and magnetic properties of the MNPs can cause deviations from this model. Thus if the MNPs differ in diameter there can be a twist of the dimer axis and slippage of MNPs as they roll over each other with the bond between them remaining parallel to the dimer axis. This can lead to additional longitudinal shear deformation of the macromolecule.

The macromolecule can also experience torsion deformation during the initial rotation of the MNP relative to the dimer axis. At the initial chaotic orientation of the magnetic moments the torsion angle is uniformly distributed from 0 to π. Under these conditions the maximal shear stress $\tau_{\mathrm{max}} = (\mu B_a \cdot d/2)/(\pi d^4/32)$ can be as high as 10 MPa for the above-discussed MNP and AMF parameters. The torsion tension in this case acts together with the compression. The fraction of the macromolecules undergoing the torsion in the real aggregates can reach 30–50% of the total number of macromolecules.

6. Conclusion

This paper provides a critical review of recent experimental studies on magneto-mechanical and related phenomena displayed by single-domain MNPs in an applied AMF and outlines potential directions of application of these phenomena in nanomedicine and drug delivery. The examples of such applications include modulation of cell responses, eradication of cancer cells, drug release from nanoparticulate carriers, activation of membrane receptors, change of activity of enzymes, and other remotely controlled processes of biomedical importance. The theoretical considerations and models describing some of these phenomena are also provided, including the dynamics of the MNP in alternating fields, solute release from the MNP polymeric corona, interaction of MNPs with lipid membranes, and magneto-mechanical deformation of biomacromolecules.

We also made an attempt to relate the magneto-mechanical phenomena that are a relatively new field of study with more established and advanced studies on magnetic hyperthermia. In this regard, one needs to take into account that the magneto-mechanical and thermic responses of the MNP systems in the applied AMF depend on multiple parameters including

the properties of the MNPs, the surrounding environment and the magnetic field characteristics. Fig. 12 presents a schematic illustration that relates these responses to the size of the MNPs, as well as the field frequency and strength. It is evident that under certain field conditions the MNP containing systems will preferentially display either thermic or magneto-mechanical responses and in other conditions both responses can be simultaneously exhibited. In addition to the size dependence of these responses one should account for the effects of the shape, the type of material used and even the method of preparation of MNPs. The picture can become even more convoluted for surface-modified MNPs, MNPs incorporated into various nanoscale structures and MNP clusters that are commonly observed in experiments. Notably, upon interaction of MNPs with serum proteins and cells, the aggregation of MNPs can also change thereby possibly affecting both the thermic and the magneto-mechanic components of their responses to the AMF. Future experimental studies should focus on further dissecting these responses and optimizing the field space and composition of the nanomaterials for their application in nanomedicine and drug delivery. The experimental and theoretical studies should also focus on better understanding the physical phenomena such as for example the effects of the pulsed fields observed by us and others that are currently not very well understood. However, there is no doubt in our view based on already available data that application of MNPs and the magneto-mechanical actuation approach in nanomedicine and drug delivery is very promising. We hope that this paper will help many academic and industrial researchers in their future successful quest into this exciting field.

Supplementary Material

Refer to Web version on PubMed Central for supplementary material.

References

1. Zhang XQ, Xu X, Bertrand N, Pridgen E, Swami A, Farokhzad OC. Interactions of nanomaterials and biological systems: implications to personalized nanomedicine. Adv Drug Deliv Rev. 2012; 64:1363–1384. [PubMed: 22917779]

2. Duncan R, Gaspar R. Nanomedicine(s) under the microscope. Mol Pharm. 2011; 8:2101–2141. [PubMed: 21974749]

3. Bamrungsap S, Zhao Z, Chen T, Wang L, Li C, Fu T, Tan W. Nanotechnology in therapeutics: a focus on nanoparticles as a drug delivery system. Nanomedicine (London). 2012; 7:1253–1271.

4. Siepmann, JR.; Siegel, RA.; Rathbone, MJ. Fundamentals and applications of controlled release drug delivery. Springer: Controlled Release Society; New York: 2012.

5. Williams HD, Trevaskis NL, Charman SA, Shanker RM, Charman WN, Pouton CW, Porter CJ. Strategies to address low drug solubility in discovery and development. Pharmacol Rev. 2013; 65:315–499. [PubMed: 23383426]

6. Jain, KK. Drug Delivery Systems. Humana; Totowa, NJ: 2008.

7. Fu K, Klibanov AM, Langer R. Protein stability in controlled-release systems. Nat Biotechnol. 2000; 18:24–25. [PubMed: 10625383]

8. Luo D, Saltzman WM. Synthetic DNA delivery systems. Nat Biotechnol. 2000; 18:33–37. [PubMed: 10625387]

9. Wang H, Jiang Y, Peng H, Chen Y, Zhu P, Huang Y. Recent progress in microRNA delivery for cancer therapy by non-viral synthetic vectors. Adv Drug Deliv Rev. 2015; 81:142–160. [PubMed: 25450259]

10. Kanapathipillai M, Brock A, Ingber DE. Nanoparticle targeting of anti-cancer drugs that alter intracellular signaling or influence the tumor microenvironment. Adv Drug Deliv Rev. 2014; 79–80:107–118.

11. Dai X, Tan C. Combination of microRNA therapeutics with small-molecule anticancer drugs: mechanism of action and co-delivery nanocarriers. Adv Drug Deliv Rev. 2015; 81:184–197. [PubMed: 25281917]

12. Thakor AS, Gambhir SS. Nanooncology: the future of cancer diagnosis and therapy. CA Cancer J Clin. 2013; 63:395–418. [PubMed: 24114523]

13. Wicki A, Witzigmann D, Balasubramanian V, Huwyler J. Nanomedicine in cancer therapy: challenges, opportunities, and clinical applications. J Control Release. 2015; 200:138–157. [PubMed: 25545217]

14. Kneidl B, Peller M, Winter G, Lindner LH, Hossann M. Thermosensitive liposomal drug delivery systems: state of the art review. Int J Nanomedicine. 2014; 9:4387–4398. [PubMed: 25258529]

15. Lu Y, Sun W, Gu Z. Stimuli-responsive nanomaterials for therapeutic protein delivery. J Control Release. 2014; 194:1–19. [PubMed: 25151983]

16. Zhang H, Wang G, Yang H. Drug delivery systems for differential release in combination therapy. Expert Opin Drug Deliv. 2011; 8:171–190. [PubMed: 21226651]

17. Xu Y, Karmakar A, Heberlein WE, Mustafa T, Biris AR, Biris AS. Multifunctional magnetic nanoparticles for synergistic enhancement of cancer treatment by combinatorial radio frequency thermolysis and drug delivery. Adv Healthcare Mater. 2012; 1:493–501.

18. Rudolf H, Silvio D, Robert M, Matthias Z. Magnetic particle hyperthermia: nanoparticle magnetism and materials development for cancer therapy. J Phys Condens Matter. 2006; 18:S2919.

19. Perera RH, Solorio L, Wu H, Gangolli M, Silverman E, Hernandez C, Peiris PM, Broome AM, Exner AA. Nanobubble ultrasound contrast agents for enhanced delivery of thermal sensitizer to tumors undergoing radiofrequency ablation. Pharm Res. 2014; 31:1407–1417. [PubMed: 23943542]

20. Sine J, Urban C, Thayer D, Charron H, Valim N, Tata DB, Schiff R, Blumenthal R, Joshi A, Puri A. Photo activation of HPPH encapsulated in "pocket" liposomes triggers multiple drug release and tumor cell killing in mouse breast cancer xenografts. Int J Nanomedicine. 2015; 10:125–145. [PubMed: 25565809]

21. Li X, Gao L, Zheng L, Kou J, Zhu X, Jiang Y, Zhong Z, Dan J, Xu H, Yang Y, Li H, Shi S, Cao W, Zhao Y, Tian Y, Yang L. The efficacy and mechanism of apoptosis induction by hypericin-mediated sonodynamic therapy in THP-1 macrophages. Int J Nanomedicine. 2015; 10:821–838. [PubMed: 25653524]

22. Puri A. Phototriggerable liposomes: current research and future perspectives. Pharmaceutics. 2013; 6:1–25. [PubMed: 24662363]

23. Kurd K, Khandagi AA, Davaran S, Akbarzadeh A. Cisplatin release from dual-responsive magnetic nanocomposites. Artif Cells Nanomed Biotechnol. 2015:1–9. [PubMed: 25822331]

24. Gazeau F, Levy M, Wilhelm C. Optimizing magnetic nanoparticle design for nanothermotherapy. Nanomedicine (London). 2008; 3:831–844.

25. Jeyadevan B. Present status and prospects of magnetite nanoparticles-based hyperthermia. J Ceram Soc Jpn. 2010; 118:391–401.

26. Laurent S, Dutz S, Hafeli UO, Mahmoudi M. Magnetic fluid hyperthermia: focus on superparamagnetic iron oxide nanoparticles. Adv Colloid Interf Sci. 2011; 166:8–23.

27. Kumar CS, Mohammad F. Magnetic nanomaterials for hyperthermia-based therapy and controlled drug delivery. Adv Drug Deliv Rev. 2011; 63:789–808. [PubMed: 21447363]

28. Yoo D, Jeong H, Preihs C, Choi J-s, Shin T-H, Sessler JL, Cheon J. Double-effector nanoparticles: a synergistic approach to apoptotic hyperthermia. Angew Chem Int Ed. 2012; 51:12482–12485.

29. Khandhar AP, Ferguson RM, Simon JA, Krishnan KM. Tailored magnetic nanoparticles for optimizing magnetic fluid hyperthermia. J Biomed Mater Res A. 2012; 100:728–737. [PubMed: 22213652]

30. Mahmoudi M, Sant S, Wang B, Laurent S, Sen T. Superparamagnetic iron oxide nanoparticles (SPIONs): development, surface modification and applications in chemotherapy. Adv Drug Deliv Rev. 2011; 63:24–46. [PubMed: 20685224]

31. Dobson J. Remote control of cellular behaviour with magnetic nanoparticles. Nat Nanotechnol. 2008; 3:139–143. [PubMed: 18654485]

32. Kim DH, Rozhkova EA, Ulasov IV, Bader SD, Rajh T, Lesniak MS, Novosad V. Biofunctionalized magnetic-vortex microdiscs for targeted cancer-cell destruction. Nat Mater. 2010; 9:165–171. [PubMed: 19946279]

33. Klyachko NL, Sokolsky-Papkov M, Pothayee N, Efremova MV, Gulin DA, Pothayee N, Kuznetsov AA, Majouga AG, Riffle JS, Golovin YI, Kabanov AV. Changing the enzyme reaction rate in magnetic nanosuspensions by a non-heating magnetic field. Angew Chem Int Ed Engl. 2012; 51:12016–12019. [PubMed: 23081706]

34. Binhi, VN. Magnetobiology: Underlying Physical Problems. Academic Press; San Diego: 2002.

35. Biological Effects of Electromagnetic Fields. Springer; Berlin: 2003.

36. Rosch, PJ.; Markov, M. Bioelectromagnetic Medicine. Marcel Dekker; New York: 2004.

37.

Health effects from radiofrequency electromagnetic fields, Report of the Independent Advisory Group on Non-ionising Radiation, 2012.

38. Ikai, A.; Afrin, R. The World of Nano-Biomechanics : Mechanical Imaging and Measurement by Atomic Force Microscopy. 1. Elsevier; Amsterdam; Boston: 2008.

39. Grissom CB. Magnetic-field effects in biology – a survey of possible mechanisms with emphasis on radical-pair recombination. Chem Rev. 1995; 95:3–24.

40. Golovin YI, Morgunov RB. A new type of magnetoplastic effects in linear amorphous polymers. Phys Solid State. 2001; 43:859–864.

41. Bingi VN, Savin AV. Effects of weak magnetic fields on biological systems: physical aspects. Physics-Uspekhi. 2003; 46:259–291.

42. Golovin YI. Magnetoplastic effects in solids. Phys Solid State. 2004; 46:789–824.

43. Milyaev VA, Binhi VN. On the physical nature of magnetobiological effects. Quantum Electron. 2006; 36:691–701.

44. Funk RH, Monsees T, Ozkucur N. Electromagnetic effects – from cell biology to medicine. Prog Histochem Cytochem. 2009; 43:177–264. [PubMed: 19167986]

45. Golovin YI, Morgunov RB. Mechanochemical reactions between defects of crystalline structure and the effect of a magnetic field on these reactions kinetics. Chem Rev. 1998; 23:23–58.

46. Salikhov, KM.; Molin, IUN.; Buchachenko, AL. Spin Polarization and Magnetic Effects in Radical Reactions. Elsevier; Akadémiai Kiadó; Amsterdam; New York Budapest, Hungary: 1984.

47. Steiner UE, Ulrich T. Magnetic-field effects in chemical-kinetics and related phenomena. Chem Rev. 1989; 89:51–147.

48. Dynamic Spin Chemistry: Magnetic Controls and Spin Dynamics of Chemical Reactions. Wiley; 1998.

49. Brocklehurst B. Magnetic fields and radical reactions: recent developments and their role in nature. Chem Soc Rev. 2002; 31:301–311. [PubMed: 12357727]

50. Alshits VI, Darinskaya EV, Koldaeva MV, Petrzhik EA. Magnetoplastic effect in nonmagnetic crystals. Discloc Solids. 2008; 14:333–437.

51. Alshits VI, Darinskaya EV, Koldaeva MV, Petrzhik EA. Magnetoplastic effect: basic properties and physical mechanisms. Crystallogr Rep. 2003; 48:768–795.

52. Golovin YI, Morgunov RB. Effect of a weak magnetic field on the state of structural defects and the plasticity of ionic crystals. J Exp Theor Phys. 1999; 88:332–341.

53. Buchachenko AL. Magnetic field-dependent molecular and chemical processes in biochemistry, genetics and medicine. Russ Chem Rev. 2014; 83:1–12.

54. Salunkhe AB, Khot VM, Pawar SH. Magnetic hyperthermia with magnetic nanoparticles: a status review. Curr Top Med Chem. 2014; 14:572–594. [PubMed: 24444167]

55. Kobayashi T. Cancer hyperthermia using magnetic nanoparticles. Biotechnol J. 2011; 6:1342–1347. [PubMed: 22069094]

56. Hergt R, Dutz S, Muller R, Zeisberger M. Magnetic particle hyperthermia: nanoparticle magnetism and materials development for cancer therapy. J Phys Condens Matter. 2006; 18:S2919–S2934.

57. Hergt R, Dutz S. Magnetic particle hyperthermia–biophysical limitations of a visionary tumour therapy. J Magn Magn Mater. 2007; 311:187–192.

58. Gupta AK, Gupta M. Synthesis and surface engineering of iron oxide nanoparticles for biomedical applications. Biomaterials. 2005; 26:3995–4021. [PubMed: 15626447]

59. Lu AH, Salabas EL, Schuth F. Magnetic nanoparticles: synthesis, protection, functionalization, and application. Angew Chem Int Ed Engl. 2007; 46:1222–1244. [PubMed: 17278160]

60. Stephen ZR, Kievit FM, Zhang M. Magnetite nanoparticles for medical MR imaging. Mater Today (Kidlington). 2011; 14:330–338. [PubMed: 22389583]

61. Ma M, Wu Y, Zhou J, Sun Y, Zhang Y, Gu N. Size dependence of specific power absorption of Fe_3O_4 particles in AC magnetic field. J Magn Magn Mater. 2004; 268:33–39.

62. Guardia P, Di Corato R, Lartigue L, Wilhelm C, Espinosa A, Garcia-Hernandez M, Gazeau F, Manna L, Pellegrino T. Water-soluble iron oxide nanocubes with high values of specific absorption rate for cancer cell hyperthermia treatment. ACS Nano. 2012; 6:3080–3091. [PubMed: 22494015]

63. Samanta B, Yan H, Fischer NO, Shi J, Jerry DJ, Rotello VM. Protein-passivated Fe(3)O(4) nanoparticles: low toxicity and rapid heating for thermal therapy. J Mater Chem. 2008; 18:1204–1208. [PubMed: 19122852]

64. Le Renard PE, Lortz R, Senatore C, Rapid JP, Buchegger F, Petri-Fink A, Hofmann H, Doelker E, Jordan O. Magnetic and in vitro heating properties of implants formed in situ from injectable formulations and containing superparamagnetic iron oxide nanoparticles (SPIONs) embedded in silica microparticles for magnetically induced local hyperthermia. J Magn Magn Mater. 2011; 323:1054–1063.

65. Sonvico F, Mornet S, Vasseur S, Dubernet C, Jaillard D, Degrouard J, Hoebeke J, Duguet E, Colombo P, Couvreur P. Folate-conjugated iron oxide nanoparticles for solid tumor targeting as potential specific magnetic hyperthermia mediators: synthesis, physicochemical characterization, and in vitro experiments. Bioconjug Chem. 2005; 16:1181–1188. [PubMed: 16173796]

66. Huang H, Delikanli S, Zeng H, Ferkey DM, Pralle A. Remote control of ion channels and neurons through magnetic-field heating of nanoparticles. Nat Nanotechnol. 2010; 5:602–606. [PubMed: 20581833]

67. Obaidat IM, Issa B, Haik Y. Magnetic properties of magnetic nanoparticles for efficient hyperthermia. Nanomaterials. 2015; 5:63–89.

68. Brezovich IA. Low frequency hyperthermia. Med Phys Monogr. 1988; 16:82–111.

69. Kikumori T, Kobayashi T, Sawaki M, Imai T. Anti-cancer effect of hyperthermia on breast cancer by magnetite nanoparticle-loaded anti-HER2 immunoliposomes. Breast Cancer Res Treat. 2009; 113:435–441. [PubMed: 18311580]

70. Amorino GP, Fox MH. Effects of hyperthermia on intracellular chloride. J Membr Biol. 1996; 152:217–222. [PubMed: 8672083]

71. Gordon RT, Hines JR, Gordon D. Intracellular hyperthermia. A biophysical approach to cancer treatment via intracellular temperature and biophysical alterations. Med Hypotheses. 1979; 5:83–102. [PubMed: 459972]

72. Ito A, Honda H, Kobayashi T. Cancer immunotherapy based on intracellular hyperthermia using magnetite nanoparticles: a novel concept of "heat-controlled necrosis" with heat shock protein expression. Cancer Immunol Immunother. 2006; 55:320–328. [PubMed: 16133113]

73. Xu Y, Mahmood M, Li Z, Dervishi E, Trigwell S, Zharov VP, Ali N, Saini V, Biris AR, Lupu D, Boldor D, Biris AS. Cobalt nanoparticles coated with graphitic shells as localized radio frequency absorbers for cancer therapy. Nanotechnology. 2008; 19:435102. [PubMed: 21832683]

74. Jordan A, Scholz R, Wust P, Schirra H, Schiestel T, Schmidt H, Felix R. Endocytosis of dextran and silan-coated magnetite nanoparticles and the effect of intracellular hyperthermia on human mammary carcinoma cells in vitro. J Magn Magn Mater. 1999; 194:185–196.

75. Amstad E, Kohlbrecher J, Muller E, Schweizer T, Textor M, Reimhult E. Triggered release from liposomes through magnetic actuation of iron oxide nanoparticle containing membranes. Nano Lett. 2011; 11:1664–1670. [PubMed: 21351741]

76. Gupta A, Kane RS, Borca-Tasciuc DA. Local temperature measurement in the vicinity of electromagnetically heated magnetite and gold nanoparticles. J Appl Phys. 2010; 108:064901.

77. Rabin Y. Is intracellular hyperthermia superior to extracellular hyperthermia in the thermal sense? Int J Hyperth. 2002; 18:194–202.

78. Andra W, d'Ambly CG, Hergt R, Hilger I, Kaiser WA. Temperature distribution as function of time around a small spherical heat source of local magnetic hyperthermia. J Magn Magn Mater. 1999; 194:197–203.

79. Hergt R, Andra W, d'Ambly CG, Hilger I, Kaiser WA, Richter U, Schmidt HG. Physical limits of hyperthermia using magnetite fine particles. IEEE Trans Magn. 1998; 34:3745–3754.

80. Giordano MA, Gutierrez G, Rinaldi C. Fundamental solutions to the bioheat equation and their application to magnetic fluid hyperthermia. Int J Hyperth. 2010; 26:475–484.

81. Keblinski P, Cahill DG, Bodapati A, Sullivan CR, Taton TA. Limits of localized heating by electromagnetically excited nanoparticles. J Appl Phys. 2006; 100

82. Hergt, R.; Andrä, W. Magnetic hyperthermia and thermoablation, Magnetism in Medicine. Wiley-VCH Verlag GmbH & Co. KGaA; 2007. p. 550-570.

83. Asin L, Ibarra MR, Tres A, Goya GF. Controlled cell death by magnetic hyperthermia: effects of exposure time, field amplitude, and nanoparticle concentration. Pharm Res. 2012; 29:1319–1327. [PubMed: 22362408]

84. Carrey J, Connord V, Respaud M. Ultrasound generation and high-frequency motion of magnetic nanoparticles in an alternating magnetic field: toward intracellular ultrasound therapy? Appl Phys Lett. 2013; 102:232404.

85. Domenech M, Marrero-Berrios I, Torres-Lugo M, Rinaldi C. Lysosomal membrane permeabilization by targeted magnetic nanoparticles in alternating magnetic fields. ACS Nano. 2013; 7:5091–5101. [PubMed: 23705969]

86. Marcos-Campos I, Asin L, Torres TE, Marquina C, Tres A, Ibarra MR, Goya GF. Cell death induced by the application of alternating magnetic fields to nanoparticle-loaded dendritic cells. Nanotechnology. 2011; 22:205101. [PubMed: 21444956]

87. Asin L, Goya GF, Tres A, Ibarra MR. Induced cell toxicity originates dendritic cell death following magnetic hyperthermia treatment. Cell Death Dis. 2013; 4:e596. [PubMed: 23598408]

88. Goya GF, Asin L, Ibarra MR. Cell death induced by AC magnetic fields and magnetic nanoparticles: current state and perspectives. Int J Hyperth. 2013; 29:810–818.

89. Creixell M, Bohorquez AC, Torres-Lugo M, Rinaldi C. EGFR-targeted magnetic nanoparticle heaters kill cancer cells without a perceptible temperature rise. ACS Nano. 2011; 5:7124–7129. [PubMed: 21838221]

90. Jadhav NV, Prasad AI, Kumar A, Mishra R, Dhara S, Babu KR, Prajapat CL, Misra NL, Ningthoujam RS, Pandey BN, Vatsa RK. Synthesis of oleic acid functionalized Fe_3O_4 magnetic nanoparticles and studying their interaction with tumor cells for potential hyperthermia applications. Colloids Surf B: Biointerfaces. 2013; 108:158–168. [PubMed: 23537834]

91. Villanueva A, de la Presa P, Alonso JM, Rueda T, Martínez A, Crespo P, Morales MP, Gonzalez-Fernandez MA, Valdés J, Rivero G. Hyperthermia HeLa cell treatment with silica-coated manganese oxide nanoparticles. J Phys Chem C. 2010; 114:1976–1981.

92. Saville SL, Qi B, Baker J, Stone R, Camley RE, Livesey KL, Ye L, Crawford TM, Thompson Mefford O. The formation of linear aggregates in magnetic hyperthermia: implications on specific absorption rate and magnetic anisotropy. J Colloid Interface Sci. 2014; 424:141–151. [PubMed: 24767510]

93. Mason, TJ.; Peters, D. Practical Sonochemistry: Power Ultrasound Uses and Applications. Woodhead Publishing; 2002.

94. Chemat F, Zill He, Khan MK. Applications of ultrasound in food technology: processing, preservation and extraction. Ultrason Sonochem. 2011; 18:813–835. [PubMed: 21216174]

95. Chandrapala J, Oliver C, Kentish S, Ashokkumar M. Ultrasonics in food processing. Ultrason Sonochem. 2012; 19:975–983. [PubMed: 22349129]

96. Yu H, Chen S, Cao P. Synergistic bactericidal effects and mechanisms of low intensity ultrasound and antibiotics against bacteria: a review. Ultrason Sonochem. 2012; 19:377–382. [PubMed: 22153228]

97. Mason TJ. Therapeutic ultrasound an overview. Ultrason Sonochem. 2011; 18:847–852. [PubMed: 21316286]

98. Ramos-de-la-Pena AM, Renard CM, Wicker L, Montanez JC, Garcia-Cerda LA, Contreras-Esquivel JC. Environmental friendly cold-mechanical/sonic enzymatic assisted extraction of genipin from genipap (Genipa americana). Ultrason Sonochem. 2014; 21:43–49. [PubMed: 23871416]

99. Mitragotri S. Devices for overcoming biological barriers: the use of physical forces to disrupt the barriers. Adv Drug Deliv Rev. 2013; 65:100–103. [PubMed: 22960787]

100. Yu ZL, Zeng WC, Lu XL. Influence of ultrasound to the activity of tyrosinase. Ultrason Sonochem. 2013; 20:805–809. [PubMed: 23207057]

101. Ninomiya K, Kawabata S, Tashita H, Shimizu N. Ultrasound-mediated drug delivery using liposomes modified with a thermosensitive polymer. Ultrason Sonochem. 2014; 21:310–316. [PubMed: 23948493]

102. Ninomiya K, Noda K, Ogino C, Kuroda S, Shimizu N. Enhanced OH radical generation by dual-frequency ultrasound with TiO_2 nanoparticles: its application to targeted sonodynamic therapy. Ultrason Sonochem. 2014; 21:289–294. [PubMed: 23746399]

103. Chen Y, Bose A, Bothun GD. Controlled release from bilayer-decorated magnetoliposomes via electromagnetic heating. ACS Nano. 2010; 4:3215–3221. [PubMed: 20507153]

104. Qiu D, An X. Controllable release from magnetoliposomes by magnetic stimulation and thermal stimulation. Colloids Surf B: Biointerfaces. 2013; 104:326–329. [PubMed: 23290769]

105. Peiris PM, Bauer L, Toy R, Tran E, Pansky J, Doolittle E, Schmidt E, Hayden E, Mayer A, Keri RA, Griswold MA, Karathanasis E. Enhanced delivery of chemotherapy to tumors using a multicomponent nanochain with radio-frequency-tunable drug release. ACS Nano. 2012; 6:4157–4168. [PubMed: 22486623]

106. Peiris PM, Abramowski A, McGinnity J, Doolittle E, Toy R, Gopalakrishnan R, Shah S, Bauer L, Ghaghada KB, Hoimes C, Brady-Kalnay SM, Basilion JP, Griswold MA, Karathanasis E. Treatment of invasive brain tumors using a chain-like nanoparticle. Cancer Res. 2015; 75:1356–1365. [PubMed: 25627979]

107. Nappini S, Bombelli FB, Bonini M, Norden B, Baglioni P. Magnetoliposomes for controlled drug release in the presence of low-frequency magnetic field. Soft Matter. 2010; 6:154–162.

108. Nappini S, Bonini M, Bombelli FB, Pineider F, Sangregorio C, Baglioni P, Norden B. Controlled drug release under a low frequency magnetic field: effect of the citrate coating on magnetoliposomes stability. Soft Matter. 2011; 7:1025–1037.

109. Nappini S, Bonini M, Ridi F, Baglioni P. Structure and permeability of magnetoliposomes loaded with hydrophobic magnetic nanoparticles in the presence of a low frequency magnetic field. Soft Matter. 2011; 7:4801–4811.

110. Banchelli M, Nappini S, Montis C, Bonini M, Canton P, Berti D, Baglioni P. Magnetic nanoparticle clusters as actuators of ssDNA release. Phys Chem Chem Phys. 2014; 16:10023–10031. [PubMed: 24487734]

111. Kim DH, Vitol EA, Liu J, Balasubramanian S, Gosztola DJ, Cohen EE, Novosad V, Rozhkova EA. Stimuli-responsive magnetic nanomicelles as multifunctional heat and cargo delivery vehicles. Langmuir. 2013; 29:7425–7432. [PubMed: 23351096]

112. Thomas CR, Ferris DP, Lee JH, Choi E, Cho MH, Kim ES, Stoddart JF, Shin JS, Cheon J, Zink JI. Noninvasive remote-controlled release of drug molecules in vitro using magnetic actuation of mechanized nanoparticles. J Am Chem Soc. 2010; 132:10623–10625. [PubMed: 20681678]

113. Hoare T, Santamaria J, Goya GF, Irusta S, Lin D, Lau S, Padera R, Langer R, Kohane DS. A magnetically triggered composite membrane for on-demand drug delivery. Nano Lett. 2009; 9:3651–3657. [PubMed: 19736912]

114. Hoare T, Timko BP, Santamaria J, Goya GF, Irusta S, Lau S, Stefanescu CF, Lin D, Langer R, Kohane DS. Magnetically triggered nanocomposite membranes: a versatile platform for triggered drug release. Nano Lett. 2011; 11:1395–1400. [PubMed: 21344911]

115. Hanus J, Ullrich M, Dohnal J, Singh M, Stepanek F. Remotely controlled diffusion from magnetic liposome microgels. Langmuir. 2013; 29:4381–4387. [PubMed: 23461732]

116. Dobson J, Cartmell SH, Keramane A, El Haj AJ. Principles and design of a novel magnetic force mechanical conditioning bioreactor for tissue engineering, stem cell conditioning, and dynamic in vitro screening. IEEE Trans Nanobiosci. 2006; 5:173–177.

117. Dobson J, Keramane A, El Haj AJ. Theory and applications of magnetic force bioreactor. Eur Cell Mater. 2002; 4:42–44.

118. Hughes S, McBain S, Dobson J, El Haj AJ. Selective activation of mechanosensitive ion channels using magnetic particles. J R Soc Interface. 2008; 5:855–863. [PubMed: 18077244]

119. Kanczler JM, Sura HS, Magnay J, Green D, Oreffo RO, Dobson JP, El Haj AJ. Controlled differentiation of human bone marrow stromal cells using magnetic nanoparticle technology. Tissue Eng A. 2010; 16:3241–3250.

120. Hughes S, Dobson J, El Haj AJ. Magnetic targeting of mechanosensors in bone cells for tissue engineering applications. J Biomech. 2007; 40(Suppl 1):S96–104. [PubMed: 17532323]

121. Hu B, El Haj AJ, Dobson J. Receptor-targeted, magneto-mechanical stimulation of osteogenic differentiation of human bone marrow-derived mesenchymal stem cells. Int J Mol Sci. 2013; 14:19276–19293. [PubMed: 24065106]

122. Hu B, Dobson J, El Haj AJ. Control of smooth muscle alpha-actin (SMA) up-regulation in HBMSCs using remote magnetic particle mechano-activation. Nanomedicine. 2014; 10:45–55. [PubMed: 23871760]

123. Hughes S, El Haj AJ, Dobson J. Magnetic micro- and nanoparticle mediated activation of mechanosensitive ion channels. Med Eng Phys. 2005; 27:754–762. [PubMed: 15985383]

124. Pankhurst QA, Thanh NTK, Jones SK, Dobson J. Progress in applications of magnetic nanoparticles in biomedicine. J Phys D Appl Phys. 2009; 42

125. Mannix RJ, Kumar S, Cassiola F, Montoya-Zavala M, Feinstein E, Prentiss M, Ingber DE. Nanomagnetic actuation of receptor-mediated signal transduction. Nat Nanotechnol. 2008; 3:36–40. [PubMed: 18654448]

126. Kim DH, Karavayev P, Rozhkova EA, Pearson J, Yefremenko V, Bader SD, Novosad V. Mechanoresponsive system based on sub-micron chitosan-functionalized ferromagnetic disks. J Mater Chem. 2011; 21:8422–8426.

127. Rozhkova EA, Novosad V, Kim DH, Pearson J, Divan R, Rajh T, Bader SD. Ferromagnetic microdisks as carriers for biomedical applications. J Appl Phys. 2009; 105

128. Rozhkova EA, Ulasov IV, Kim DH, Dimitrijevic NM, Novosad V, Bader SD, Lesniak MS, Rajh T. Multifunctional nano-bio materials within cellular machinery. Int J Nanosci. 2011; 10:899. [PubMed: 23105163]

129. Vitol EA, Novosad V, Rozhkova EA. Multifunctional ferromagnetic disks for modulating cell function. IEEE Trans Magn. 2012; 48:3269–3274. [PubMed: 23766544]

130. Vitol EA, Novosad V, Rozhkova EA. Microfabricated magnetic structures for future medicine: from sensors to cell actuators. Nanomedicine (London). 2012; 7:1611–1624.

131. Dobson J. Cancer therapy: a twist on tumour targeting. Nat Mater. 2010; 9:95–96. [PubMed: 19946278]

132. Majouga A, Sokolsky-Papkov M, Kuznetsov A, Lebedev D, Efremova M, Beloglazkina E, Rudakovskaya P, Veselov M, Zyk N, Golovin Y, Klyachko N, Kabanov A. Enzyme-functionalized gold-coated magnetite nanoparticles as novel hybrid nanomaterials: synthesis, purification and control of enzyme function by low-frequency magnetic field. Colloids Surf B: Biointerfaces. 2015; 125:104–109. [PubMed: 25460600]

133. Klibanov AM. Enzyme stabilization by immobilization. Anal Biochem. 1979; 93:1–25. [PubMed: 35035]

134. Klibanov AM, Samokhin GP, Martinek K, Berezin IV. Enzymatic mechanochemistry: a new approach to studying the mechanism of enzyme action. Biochim Biophys Acta. 1976; 438:1–12. [PubMed: 938678]

135. Rios C, Longo J, Zahouani S, Garnier T, Vogt C, Reisch A, Senger B, Boulmedais F, Hemmerle J, Benmlih K, Frisch B, Schaaf P, Jierry L, Lavalle P. A new biomimetic route to engineer enzymatically active mechano-responsive materials. Chem Commun. 2015; 51:5622–5625.

136. Hammes-Schiffer S, Benkovic SJ. Relating protein motion to catalysis. Annu Rev Biochem. 2006; 75:519–541. [PubMed: 16756501]

137. Puchner EM, Gaub HE. Single-molecule mechanoenzymatics. Annu Rev Biophys. 2012; 41:497–518. [PubMed: 22577826]

138. Reiner JE, Balijepalli A, Robertson JW, Campbell J, Suehle J, Kasianowicz JJ. Disease detection and management via single nanopore-based sensors. Chem Rev. 2012; 112:6431–6451. [PubMed: 23157510]

139. Wen JD, Lancaster L, Hodges C, Zeri AC, Yoshimura SH, Noller HF, Bustamante C, Tinoco I. Following translation by single ribosomes one codon at a time. Nature. 2008; 452:598–603. [PubMed: 18327250]

140. Golovin YI, Klyachko NL, Golovin DY, Efremova MV, Samodurov AA, Sokolski-Papkov M, Kabanov AV. A new approach to the control of biochemical reactions in a magnetic nanosuspension using a low-frequency magnetic field. Tech Phys Lett. 2013; 39:240–243.

141. Golovin YI, Gribanovskii SL, Golovin DY, Klyachko N, Kabanov A. Single-domain magnetic nanoparticles in an alternating magnetic field as mediators of local deformation of the surrounding macromolecules. Phys Solid State. 2014; 56:1342–1351.

142. Golovin YI, Gribanovskii SL, Klyachko N, Kabanov A. Nanomechanical control of the activity of enzymes immobilized on single-domain magnetic nanoparticles. Tech Phys. 2014; 59:932–935.

143. Noy, A. Handbook of Molecular Force Spectroscopy. Springer; New York, NY: 2008.

144. Yanagida, T.; Ishii, Y. Single Molecule Dynamics in Life Science. Wiley-VCH; Weinheim: 2009.

145. Suresh S. Biomechanics and biophysics of cancer cells. Acta Biomater. 2007; 3:413–438. [PubMed: 17540628]

146. Oberhauser, AF. Single-molecule Studies of Proteins. Springer; New York: 2013.

147. Mizuki T, Watanabe N, Nagaoka Y, Fukushima T, Morimoto H, Usami R, Maekawa T. Activity of an enzyme immobilized on superparamagnetic particles in a rotational magnetic field. Biochem Biophys Res Commun. 2010; 393:779–782. [PubMed: 20171160]

148. Zhang E, Kircher MF, Koch M, Eliasson L, Goldberg SN, Renstrom E. Dynamic magnetic fields remote-control apoptosis via nanoparticle rotation. ACS Nano. 2014; 8:3192–3201. [PubMed: 24597847]

149. Tomasini MD, Rinaldi C, Tomassone MS. Molecular dynamics simulations of rupture in lipid bilayers. Exp Biol Med (Maywood). 2010; 235:181–188. [PubMed: 20404033]

150. Golovin YI, Klyachko N, Gribanovskii SL, Golovin DY, Samodurov AA, Majouga A, Sokolsky-Papkov M, Kabanov A. Nanomechanical control of properties of biological membranes achieved by rodlike magnetic nanoparticles in a superlowfrequency magnetic field. Tech Phys Lett. 2015; 41:455–457.

151. Golovin YI, Klyachko NL, Sokolsky-Papkov M, Kabanov AV. Single-domain magnetic nanoparticles as force generators for the nanomechanical control of biochemical reactions by low-frequency magnetic fields. Bull Russ Acad Sci Phys. 2013; 77:1350–1359.

152. Callender R, Dyer RB. The dynamical nature of enzymatic catalysis. Acc Chem Res. 2015; 48:407–413. [PubMed: 25539144]

153. Henzler-Wildman KA, Lei M, Thai V, Kerns SJ, Karplus M, Kern D. A hierarchy of timescales in protein dynamics is linked to enzyme catalysis. Nature. 2007; 450:913–916. [PubMed: 18026087]

154. Eisenmesser EZ, Millet O, Labeikovsky W, Korzhnev DM, Wolf-Watz M, Bosco DA, Skalicky JJ, Kay LE, Kern D. Intrinsic dynamics of an enzyme underlies catalysis. Nature. 2005; 438:117–121. [PubMed: 16267559]

155. Hoffman BD, Grashoff C, Schwartz MA. Dynamic molecular processes mediate cellular mechanotransduction. Nature. 2011; 475:316–323. [PubMed: 21776077]

Appendix A. Supplementary data

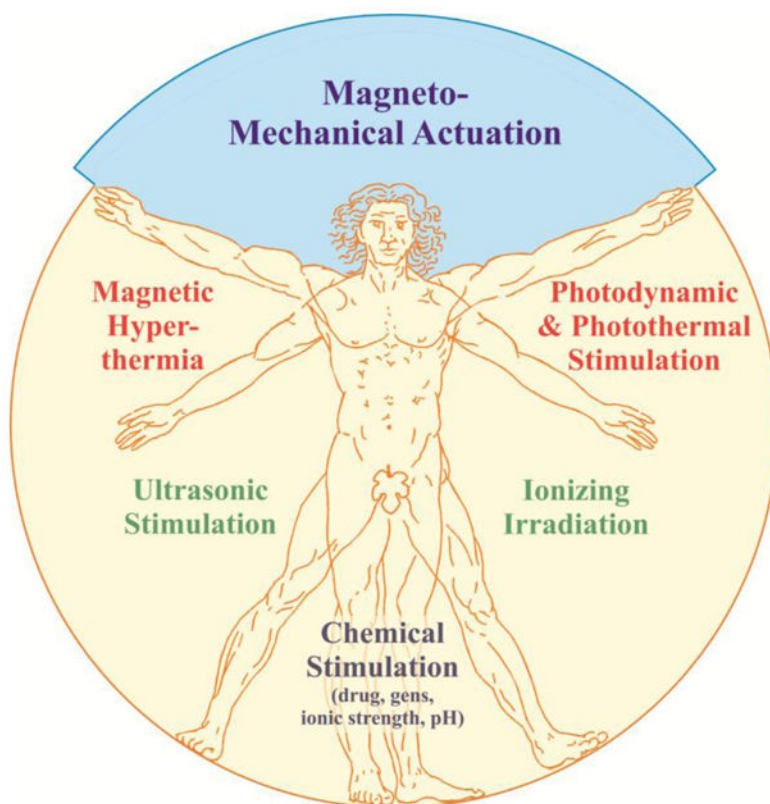Supplementary data to this article can be found online at http://dx.doi.org/10.1016/j.jconrel. 2015.09.038.

Fig. 1.
Various strategies for remote actuation of nanomedicine and drug delivery systems.
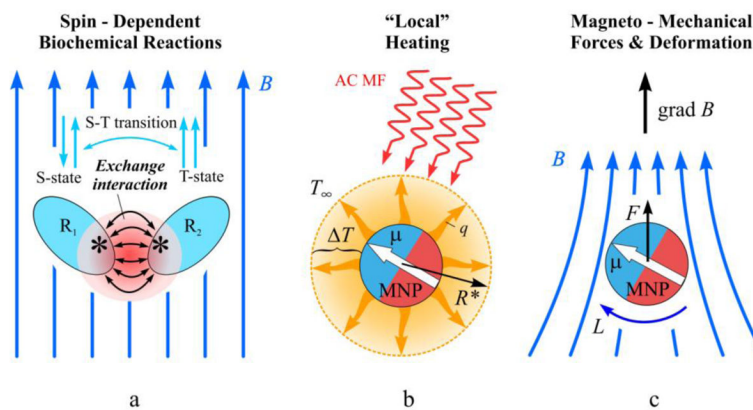
Fig. 2.
Three different routes of influencing biochemical processes using magnetic field: (a) spin-dependent, (b) thermal (magnetic hyperthermia), and (c) magneto-mechanical. R_1 and R_2 radicals; MNP – magnetic nanoparticle; μ – the magnetic moment of this nanoparticle; B – induction of the magnetic field; T_∞ – temperature at the infinite distance; T – local temperature increase at the surface of the MNP; R^* – radius of the thermal diffusion; F and L force and torque, respectively, acting upon MNP in a non-uniform magnetic field.
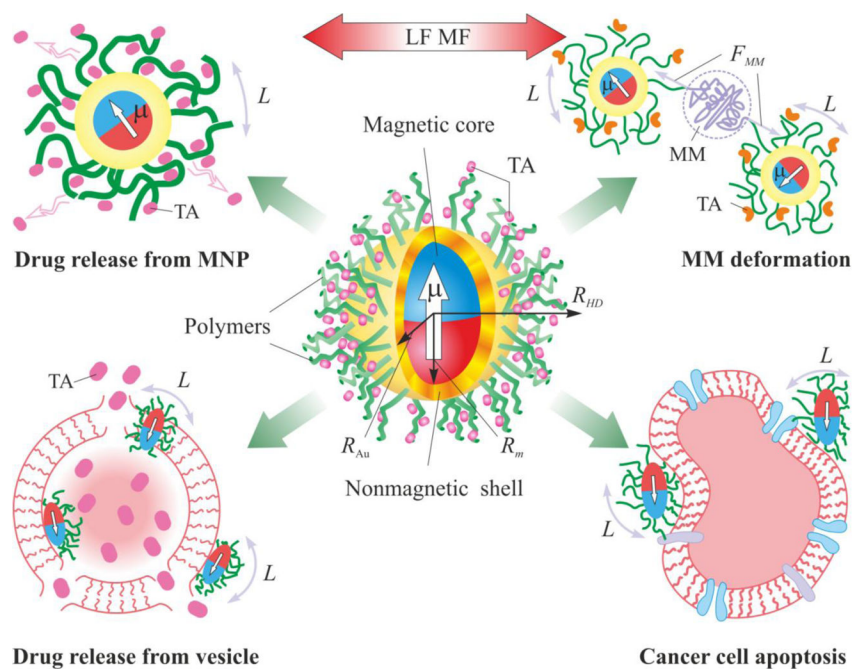
Fig. 3.
Schematic presentation of currently explored directions in nanomedicine and drug delivery that exploit magneto-mechanical actuation of functionalized MNPs in a low frequency magnetic field. Abbreviations correspond to a low frequency AMF (LF MF); therapeutic agent (TA), the magnetic moment of (μ), the torque applied to MNP (L), the macromolecule (*e.g.* enzyme) attached to MNP (MM), the magneto-mechanical force causing macromolecule deformation (F_{MM}). A schematic of functionalized MNP is presented having a superparamagnetic core of a radius R_m, a solid shell (*e.g.* gold) of a radius R_{Au} and water-soluble polymeric corona. The hydrodynamic radius of the functionalized MNP is R_{HD}.
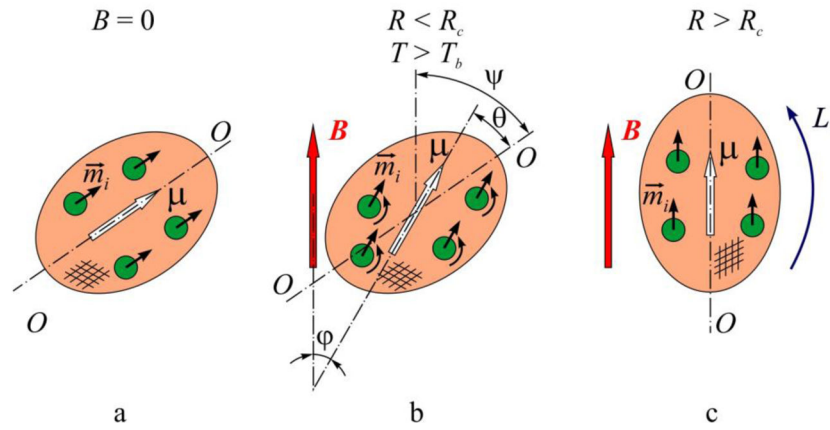
Fig. 4.
A single domain MNP in the external magnetic field B. Left to right – pristine state, Neel relaxation, and Brown relaxation. O–O is the axis of easy magnetization, m_i and μ– the magnetic moments of the i-th atom and the nanoparticle, respectively, L – torque, T_b – blocking temperature of the magnetic moments of the atoms.
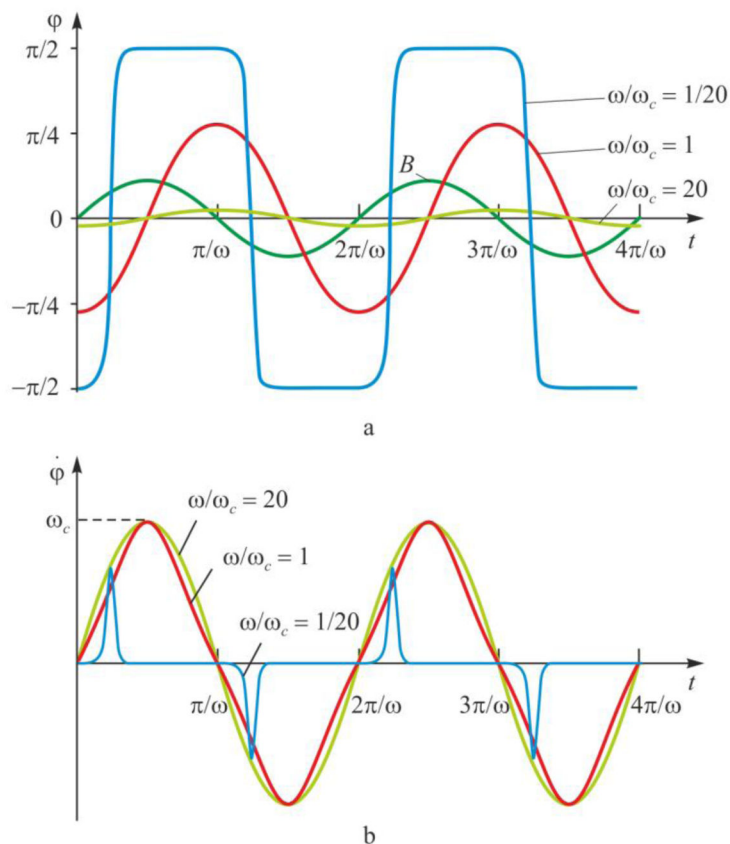
Fig. 5.
Steady-state dependencies on the current time t of the (a) induction of the AMF B and angular position of the magnetization vector μ; (b) instant angular velocity $\dot{\varphi}$ of the MNP at different ratios ω/ω_c (where $\omega_c = \mu B/(6\eta V_{HD})$).
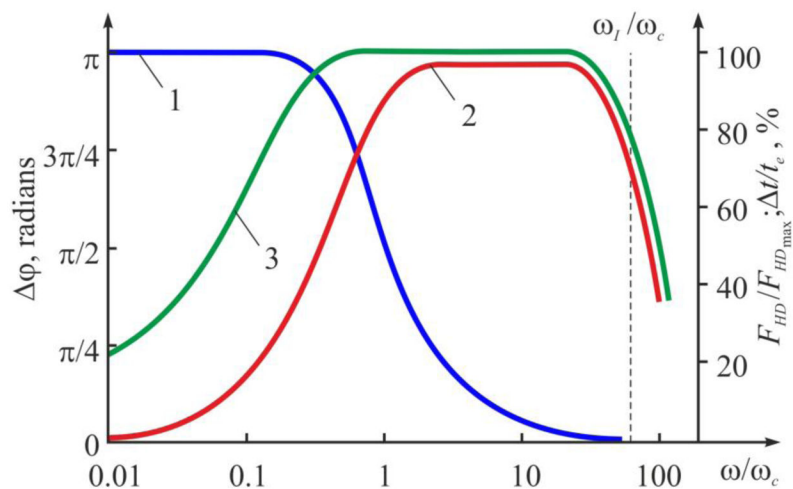
Fig. 6.
Steady-state dependencies of the amplitude of oscillation of MNP, φ **(1)**, relative hydrodynamic force, $F_{HD} / F_{HD\text{max}}$ **(2)** and relative time of movement, t / t_e **(3)** on the cyclic frequency of the external AMF ω, normalized by the characteristic frequency $\omega_c = \mu B / (6\eta V_{HD})$.
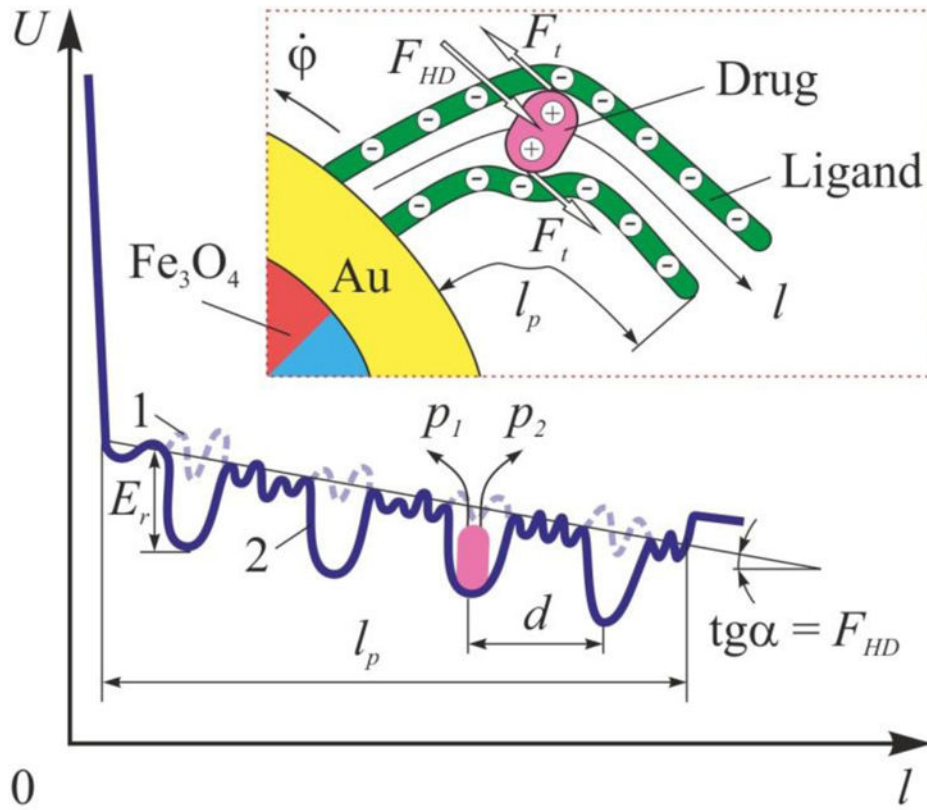
Fig. 7.
The profile of the energy of (1) van der Waals interactions, or (2) electrostatic interaction or hydrogen bond interactions of a therapeutic molecule with polymer chains of the length l_p. The insert presents a schematic of the functionalized MNP. The rest of the abbreviations are presented in the text.
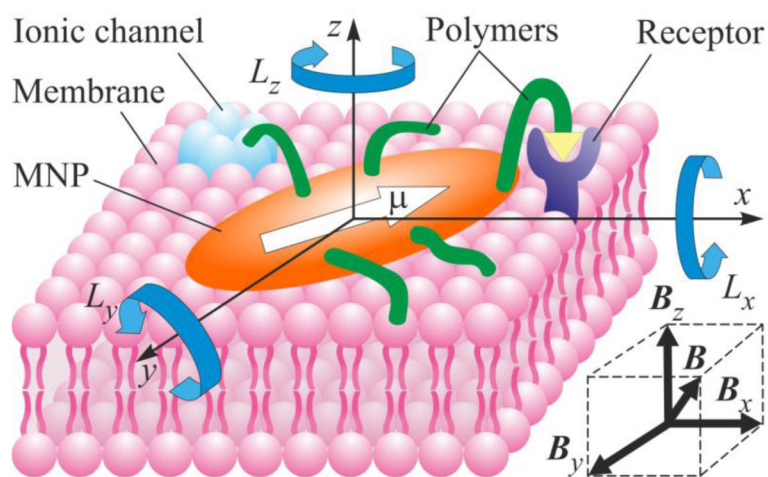
Fig. 8.
Schematic representation of interactions of a rod-like MNP having a magnetic moment $\boldsymbol{\mu}$ with the lipid membrane upon application of the external AMF having induction $\boldsymbol{B}$. The vector of induction is directed arbitrary to the membrane surface and $\boldsymbol{\mu}$ B_x, B_y, B_z и L_x, L_y, and L_z are projections of the induction and torque, respectively.
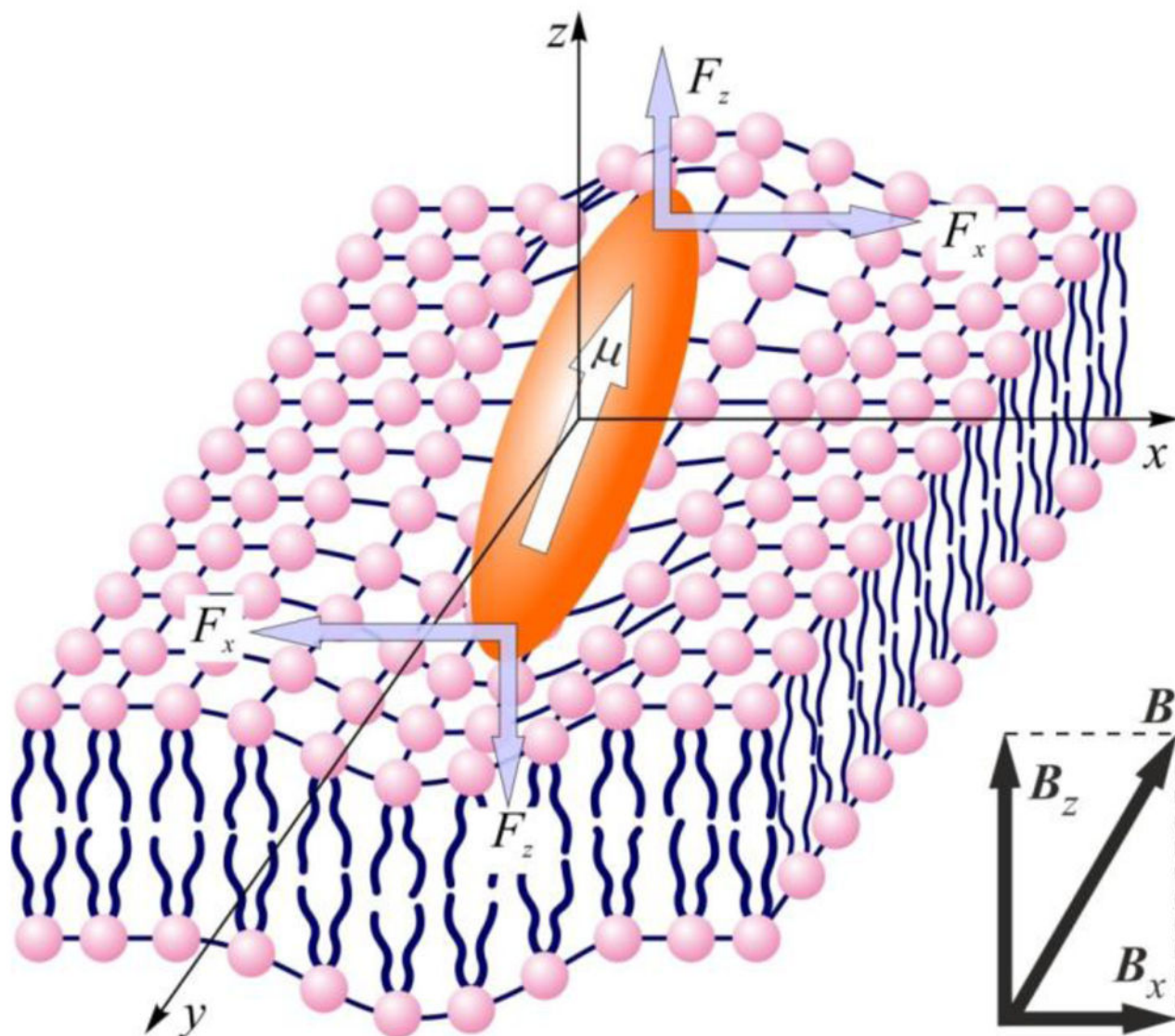
Fig. 9.
Schematic demonstration of the forces and deformations that appear in the membrane upon action of the MNP and an AMF. Weak adhesive forces connect the MNP and membrane.
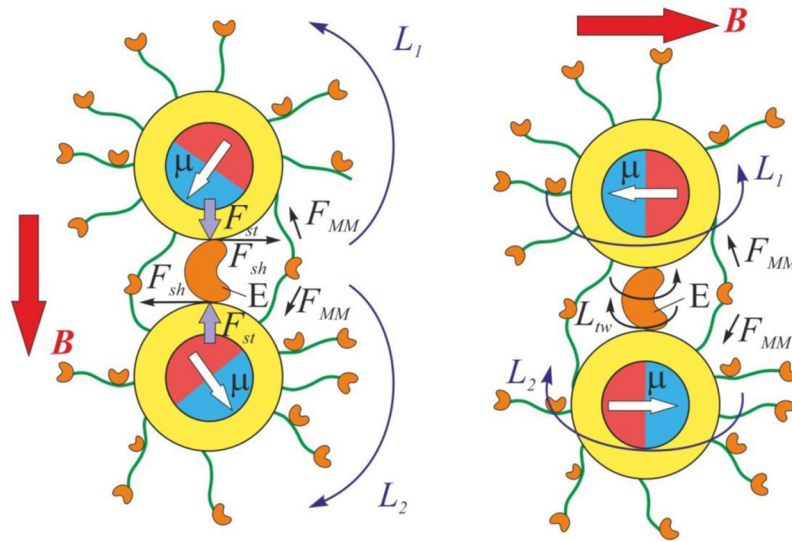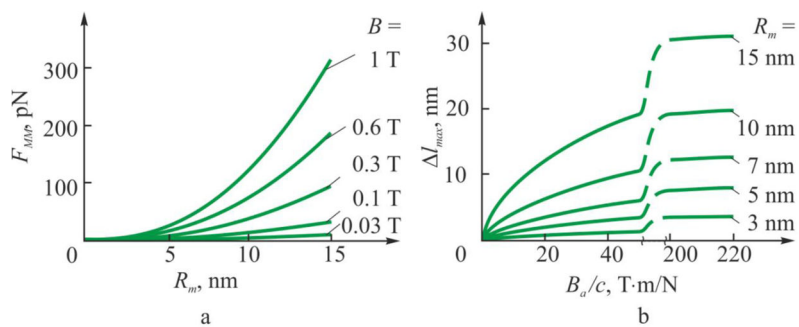
Fig. 10.
Magneto-mechanical forces and deformation in immobilized macromolecules.

Fig. 11.
Force and deformation of the system "linker–enzyme–linker" caused by the effect of the AMF depending on the main parameters of the system. (a) Dependence of maximal achievable force applied to the enzyme on the magnetic radius of MNP at various fields. (b) Dependence of maximal deformation on the ratio B_a/c for different radii of the magnetic core ($\delta = 5$ nm, $\theta_0 = 90°$).
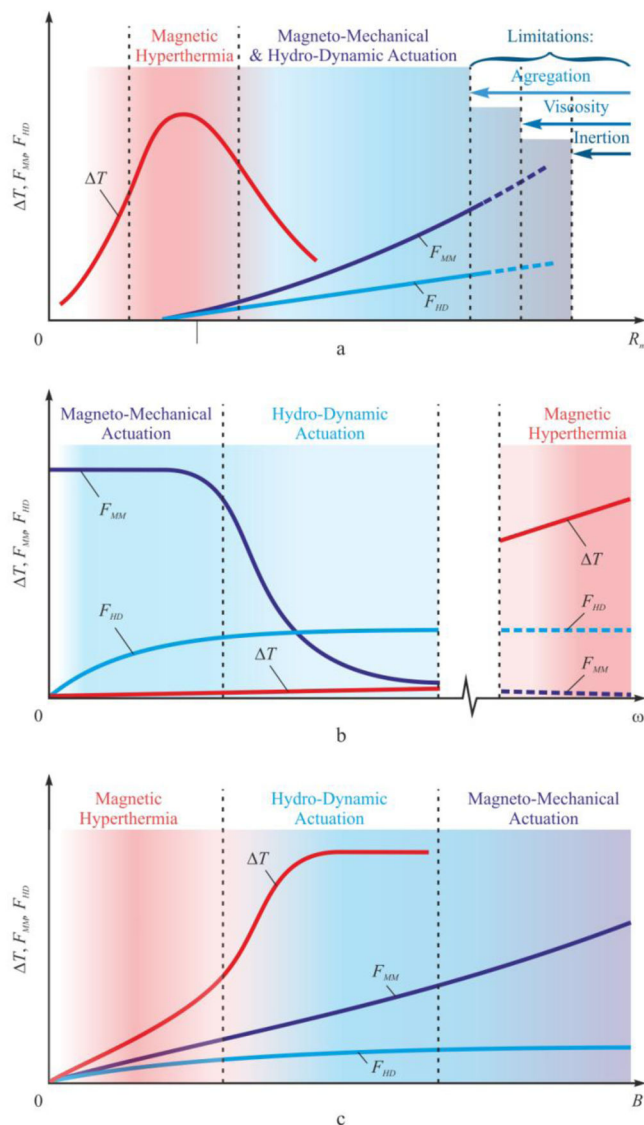Based on Ref. [141].

Fig. 12.

The areas of optimal conditions for magnetic hyperthermia (ΔT), and magneto-mechanical (F_{MM}) and/or hydrodynamic (F_{HD}) actuation as functions of (a) the magnetic core radius (R_m), (b) the field frequency ($\omega = 2\pi f$) and (c) field strength (**B**).

Table 1

Characteristic forces and the field values corresponding to the onset of some mechano-chemical processes in living organisms [38,144,145].

Process	Force, pN	Required field B,[a] mT
Activation of various ion channels	0.2–10	0.6–30
Protein–protein interaction	1–10	3–30
Activation of membrane receptors	10–50	30–150
Rupture of attraction between lipid membrane and membrane protein	30–50	90–150
Antibody–antigen interaction	10–100	30–300
Protein molecule unfolding	20–100	60–300
Ligand–receptor interaction	~1000	3000
Lipid–protein interaction	50–100	150–300
Rupture of a bilayer membrane (at $R = 10$ nm)	60–150	180–450
Breakage of a covalent bond	10^3–$5 \cdot 10^3$	3000–15,000

[a]The estimated values of the field B required to induce magneto-mechanical disruption of the processes and interactions presented in the table as estimated based on Eq. (6) below.